

THE
ASTROPHYSICAL JOURNAL
AN INTERNATIONAL REVIEW OF SPECTROSCOPY
AND ASTRONOMICAL PHYSICS

VOLUME XXVII

MAY 1908

NUMBER 4

AN INVESTIGATION OF THE FORTY-INCH OBJECTIVE
OF THE YERKES OBSERVATORY

By PHILIP FOX

Shortly after publishing¹ his method for testing objectives, Professor Hartmann directed a letter to Professor Hale, reviewing briefly the results of his investigations on the Potsdam objectives and on the 27-inch Grubb and 12-inch Clark objectives in Vienna, and speaking of the interest that would be felt in an investigation of the 40-inch objective. He concluded by saying, "Ich würde gern bereit sein, die nöthigen Messungen und Rechnungen auszuführen, wenn Sie mir nur zwei photographische Aufnahmen mit dem 40-inch Refractor anfertigen lassen wollten."

In compliance with this request, the extra-focal exposures were made by Professor Barnard on February 1, 1902. Professor Hartmann communicated the results of his measurements to Mr. Hale in April of the same year. Positives from these plates have been measured also by Mr. Ichinohe, recently fellow at this observatory, who further measured a pair of plates exposed by Mr. Jordan in April of 1906. In the table on the following page will be found the results of the measurements of the early plates. The agreement is fairly close.

In discussing the results Hartmann wrote: "So viel man aus diesen wenigen Punkten erkennen kann, ist das Objectiv ganz vorzüglich. Von $r=26$ cm bis zum Rande besteht nur eine Focusdifferenz von

¹ *Astrophysical Journal*, 12, 46, 1900.

0.05 in.; ich habe eine so kleine Differenz noch bei keinem anderen Objectiv gefunden. Dass die Mitte des Objectivs etwas kürzere Brennweite hat, ist bei der geringeren Apertur der betreffenden Strahlenkegel unschädlich. Uebrigens würde sich dieser Fehler durch nochmaliges Nachpoliren der Mitte, so dass das Objectiv dort etwas flacher würde, leicht beseitigen lassen."

RADIUS OF ZONE mm	FOCAL SCALE READINGS	
	Hartmann Inches	Ichinohe Inches
100.....	8.860	8.877
140.....	8.911	8.939
260.....	9.016	9.010
300.....	9.047	9.048
420.....	9.060	9.06
460.....	9.023	9.039
490.....	9.022	9.025

Hartmann, however, considered the investigation incomplete because so few zones were included. It is evident that undetected

90°

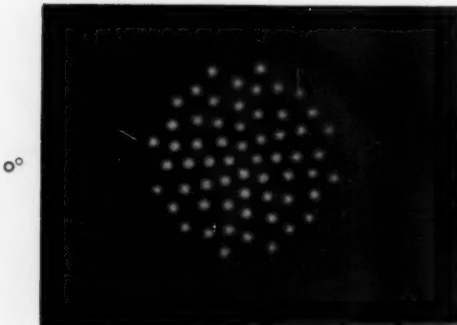


FIG. 1.—Extra-focal Star Images for the Zonal Investigation.

irregularities might lie in the gap between $r=300$ and $r=420$. The writer had the pleasure of working with Professor Hartmann in Potsdam for a few weeks in 1906, and measured some of the plates made in the tests of the 80-cm Potsdam refractor. At that time Hartmann urged the need of a more thorough test of the 40-inch objective. This investigation was therefore inaugurated.

The method first published in this *Journal* (*loc. cit.*) was later more fully developed in the *Zeitschrift für Instrumentenkunde* (24, I, 33, 97, 1904). As it has recently been referred to somewhat in detail in this *Journal* by Plaskett,¹

¹ *Astrophysical Journal*, 25, 195, 1907; also *Journal of the Royal Astronomical Society of Canada*, I, 104, 297, 1907.

FORTY-INCH YERKES OBJECTIVE

239

TABLE I
ZONAL FOCI

RADIUS OF ZONE	ϕ	OBJECTIVE ALONE							OBJECTIVE WITH CORRECTING LENS			
		1		2		3		4	5	5 (S)	Mean	6
		mm	mm	mm	mm	mm	mm	mm	mm	mm	mm	mm
490	{ 15° 105	210.23	210.04	206.11	211.40	211.39	210.92	209.83	209.83	209.83	209.83	262.64
480	{ 75 165	207.84	207.98	204.20	209.93	209.40	209.41	207.87	207.87	207.87	207.87	265.22
460	{ 45 135	206.92	207.63	204.36	210.04	209.65	209.74	207.72	207.72	207.72	207.72	264.11
440	{ 60 150	207.74	207.32	204.73	210.58	210.66	210.42	208.21	208.21	208.21	208.21	264.09
420	{ 30 120	207.40	207.54	205.03	211.04	211.02	211.10	208.41	208.41	208.41	208.41	264.09
400	{ 0 90	206.92	206.76	204.50	210.48	210.64	210.68	207.86	207.86	207.86	207.86	264.09
370	{ 15 105	206.37	206.76	204.21	210.38	210.81	210.78	207.71	207.71	207.71	207.71	264.09
340	{ 67.5 157.5	206.05	205.29	203.41	209.73	210.25	210.57	206.95	206.95	206.95	206.95	264.09
310	{ 45 135	204.61	205.37	202.48	209.71	209.63	209.92	206.36	206.36	206.36	206.36	264.09
280	{ 0 90	205.69	205.46	203.16	210.33	209.98	210.10	206.92	206.92	206.92	206.92	264.09
250	{ 22.5 112.5	206.11	205.88	203.30	209.55	210.78	211.02	207.12	207.12	207.12	207.12	264.09
230	{ 60 150	205.03	205.54	203.04	210.59	210.40	209.92	206.92	206.92	206.92	206.92	264.09
170	{ 0 90	201.67	202.24	199.77	205.73	206.38	206.64	203.16	203.16	203.16	203.16	264.09
140	{ 45 135	203.21	204.01	201.07	209.57	208.94	208.39	205.36	205.36	205.36	205.36	264.09
70	{ 0 90	201.53	200.66	198.50	203.09	202.66*	201.08*	201.29	201.29	201.29	201.29	264.09

* Poor images.

in his thorough investigation of the 15-inch objective of the Dominion Observatory, I shall not review it here. The perforated diaphragm for the present zonal test had sixty holes located at the corners of squares on fifteen different zones. The arrangement can be well seen in Fig. 1, which is a reproduction of one of the plates measured. The holes were two centimeters in diameter. Of the several pairs of exposures made, five were suitable for measurement and enter in the discussion. Also two pairs were made with the photographic correcting lens of the Bruce spectrograph in position.

During the exposures the telescope was carefully guided by means of the long-focus finder ($f=62$ ft.). When necessary the telescope was moved with the slow-motion motors. The images show no appreciable guiding errors.

The results obtained from the measurement and reduction of the plates are given in Table I. The first column gives the radius of the zones; the second gives the position angles of the holes in the diaphragm, which are measured counter-clockwise with 0° on the edge of objective away from the pier. Columns headed 1, 2, 3, 4, and 5 give the focal scale readings in millimeters for the five pairs of plates. Column 5 (S) gives results obtained from plate 5 by Professor Slocum of Brown University, volunteer research assistant at this observatory in the summer of 1907. The excellent agreement of the two sets of measurements on plate 5 speak well for the accuracy of the method. As the plates were exposed at different temperatures, there is considerable variation among the different plates. The mean values of column 9 do not include results in column 5 (S). The results are shown graphically in Fig. 2. Small values of the focal setting indicate short focal length. I have not drawn a curve for Slocum's results but have indicated them with circles.

It is at once apparent that the center of the objective is of appreciably shorter focal length than the edge, confirming the earlier extra-focal investigations. It is further seen that certain of the curves show gradual shortening of the focus with approach toward the center, while others, Nos. 4 and 5, show but little shortening until the zone $r=210$ mm is reached.

It is interesting to see what effect the variations in form of the curve has^e on the image. Hartmann has introduced a criterion " T ," for

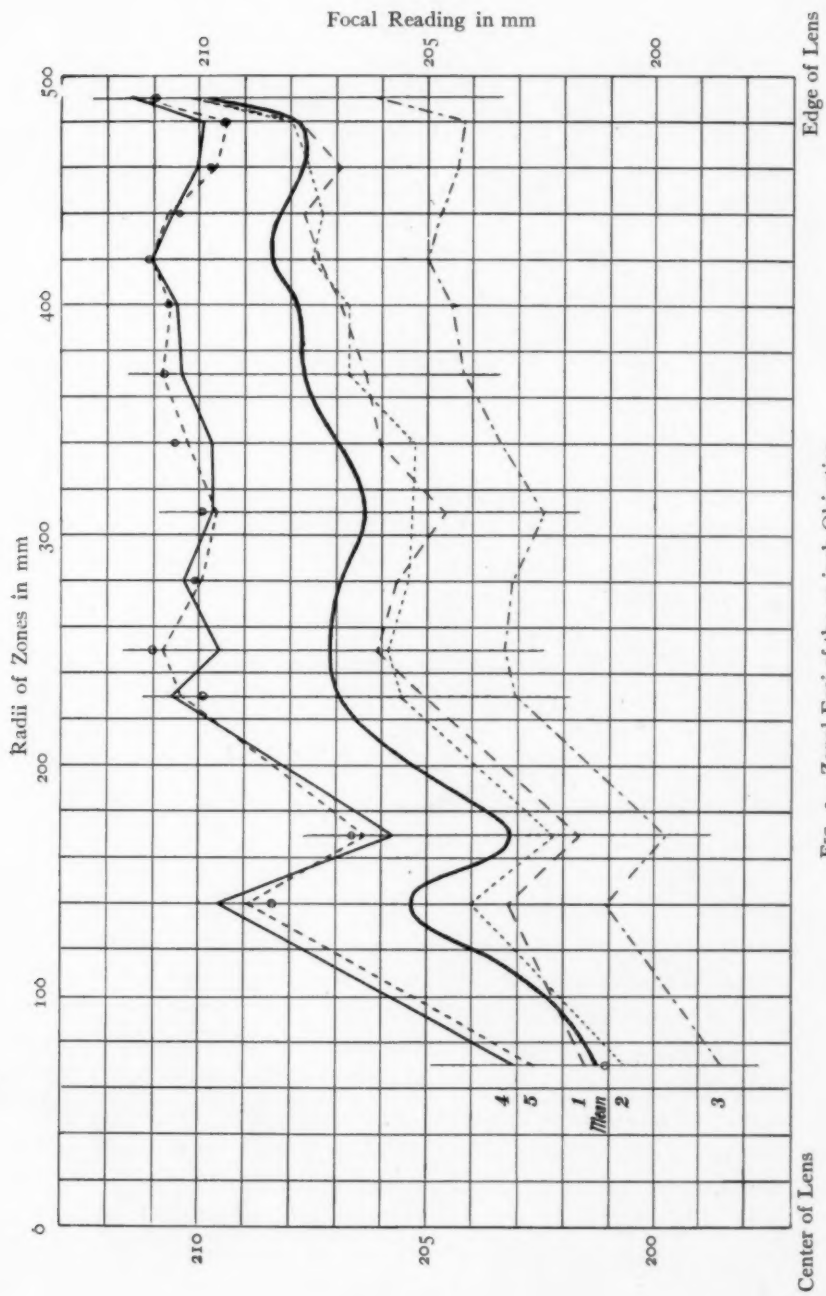


FIG. 2.—Zonal Foci of the 40-inch Objective

comparing objectives, defined as the weighted mean diameter, expressed in hundred-thousandths of the focal length, of the cones of light from the various zones in that plane, F_o , where the circle of light containing all of the converging pencils is smallest. Weights are given according to the light-gathering power of the zones, that is, according to their radii, r .

$$T = \frac{100,000}{F_m} \frac{\Sigma rd}{\Sigma r} = \frac{200,000}{F_m^2} \frac{\Sigma r^2(F - F_o)}{\Sigma r}$$

Hartmann states that after locating the plane F_o we might use the diameter of this smallest circle containing all the light, that is, the maximum of d , as a criterion of the quality of the objective; but it would be more nearly correct to take the mean value of d , for it is

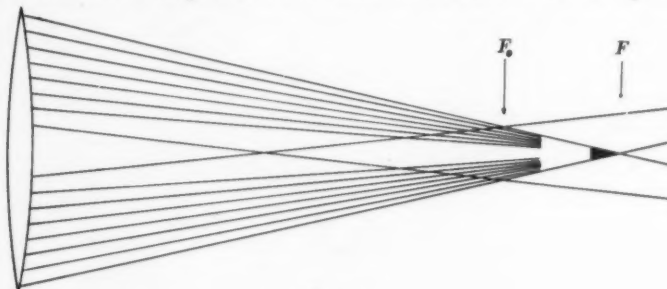


FIG. 3

possible that the maximum of d might depend on a small zone weak in light-gathering power. But this, too, while surely giving a better test, might give results poorly indicating the quality of the objective. I have shown such a case (of course very greatly exaggerated) in Fig. 3, where all the zones except one near the center give a common focus. It is evident that in practical work with such an objective the focus used would be at F (and not at F_o), and it would be manifestly unfair to judge it by even the mean diameter of the cones in the plane F_o . To free F_o from its dependence on any one zone I have sought that plane for F_o where the mean weighted diameter of the converging cones, Σrd , is a minimum. I had thought that this plane might be determined by taking the mean of the several foci, weighting them according to the angle of the cone and according to the light-gathering power; that is, roughly

$$F_o = \frac{\Sigma r^2 F}{\Sigma r^2}$$

TABLE II
CRITERION T

PLATE NUMBER	F_o		T		ZENITH DISTANCE	TEMPERA- TURE	STAR	1907
	Hartmann	$F_o = \frac{\Sigma r^2 d}{\Sigma r^2}$	Hartmann	$F_o = \frac{\Sigma r^2 d}{\Sigma r^2}$				
1.....	268.03	207.12	207.12	0.298	0.239	35°	-1.0 C	Feb. 9
2.....	268.03	207.18	207.30	0.276	0.233	53	-1.0	Feb. 9
3.....	204.48	204.27	204.27	0.162	0.160	31	-6.0	March 3
4.....	269.94	210.31	210.31	0.125	0.109	14	+12.2	June 8
5.....	210.10	210.30	210.60	0.145	0.136	9	+20.0	June 15
5 (S).....	269.69	210.26	210.50	0.162	0.123	9	+20.0	June 15
6.....	261.16		0.264			25	+4.0	March 16
7.....	263.31		0.254			25	+19.5	June 15

One or two trials for F_o on either side of this plane advancing in steps of 0.1 mm will give the plane where Σrd is a minimum. Table II gives F_o according to Hartmann's formula, $F_o = \frac{\Sigma r^2 F}{\Sigma r^2}$, and F_o where Σrd = a minimum, also T for these three different values of F_o . In computing T I have taken Barnard's value, 19,354 mm, for the focal length F_m . I have added columns giving the star's name, the date of exposure, the zenith distance at the middle of the exposure, and the temperature. I should remark that the two exposures on plate 1 were separated by 1^h32^m, so that here the zenith distance is a mean of 41° 5 and 28°.

Hartmann classes an objective as, "pre-eminently good," when T is less than 0.5; here all of the different pairs of images give values well within this class, although there is a considerable range in the values. Plates 4 and 5 are especially good. I have compared the values of T , having regard to the zenith distances, to see if the variation could be explained by flexure of the objective, and find that the performance seems to vary with the zenith distance, the object-glass giving better results when it lies horizontally. A more thorough investigation would be necessary to settle this point definitely. A series of plates on a star transiting near the zenith, say *Capella*, following the star from the zenith to the horizon should decide the question. Should this indicated relation be confirmed, it would seem that even if mechanical difficulties could be lightly overcome, refractors cannot be constructed of notably greater dimensions than the 40-inch with the hope of uniform performance at all altitudes.

With the spectrographic correcting lens in position, I found the same type of curve of zonal errors, although the curves are somewhat steeper. The focal settings are given in Table I, in columns headed 6 and 7, and are shown graphically in Fig. 4. The values of T given in Table II are not greatly different from those of the objective alone, and put the combination in the class "excellent."

With the holes in the diaphragm in a square configuration for each zone, the focal length may be determined in two planes perpendicular to each other, and any difference in the two will be due to astigmatism, if we disregard the disturbing effect of possible local errors. In Table I, I have given only the mean of the focal lengths in the two planes; this, subtracted from the two individual determinations, gives

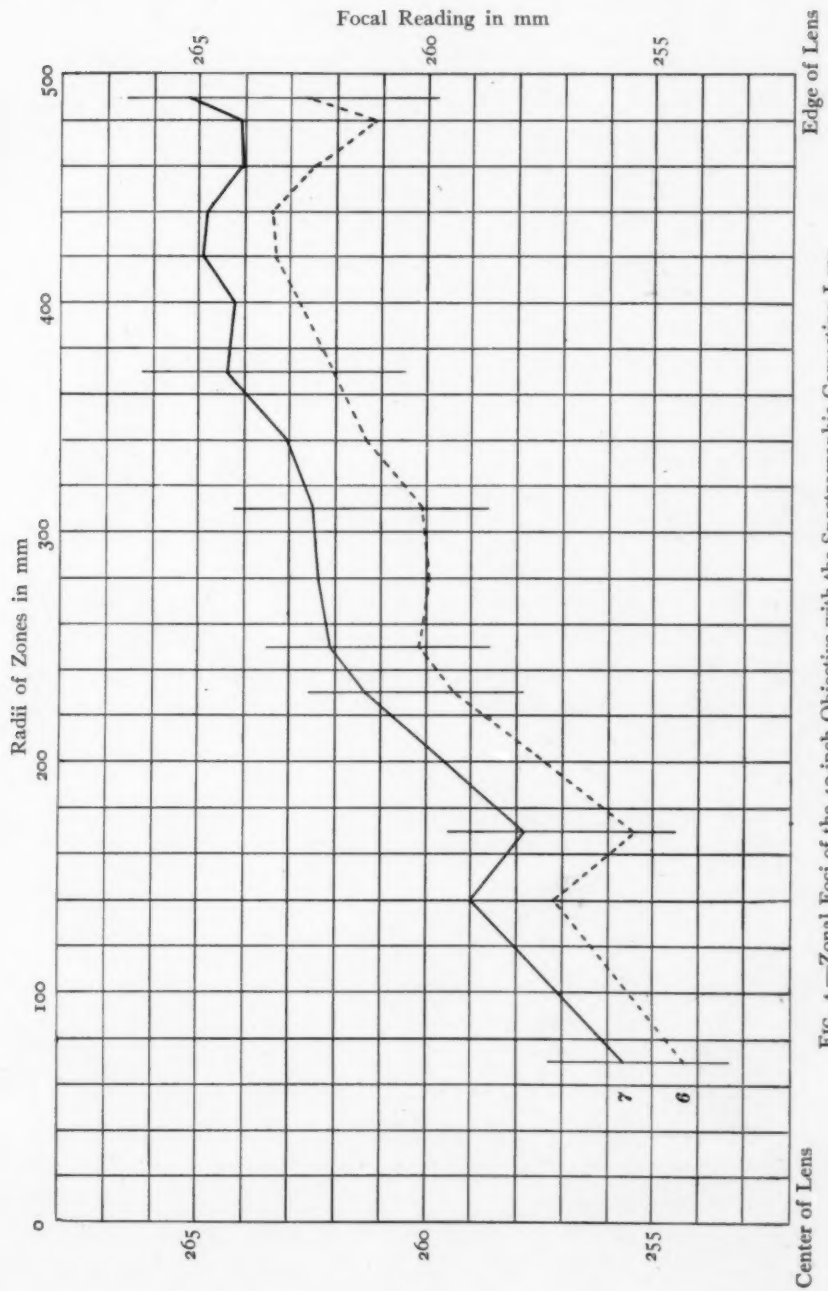


FIG. 4.—Zonal Foci of the 40-inch Objective with the Spectrographic Correcting Lens

the astigmatic errors presented in Table III. Errors for $\phi + 180^\circ$ are identical with those for ϕ , those for $\phi + 90^\circ$ and $\phi + 270^\circ$ have the opposite sign. These errors are shown graphically in Fig. 5. The negative values, those shorter than the mean for the zone, are

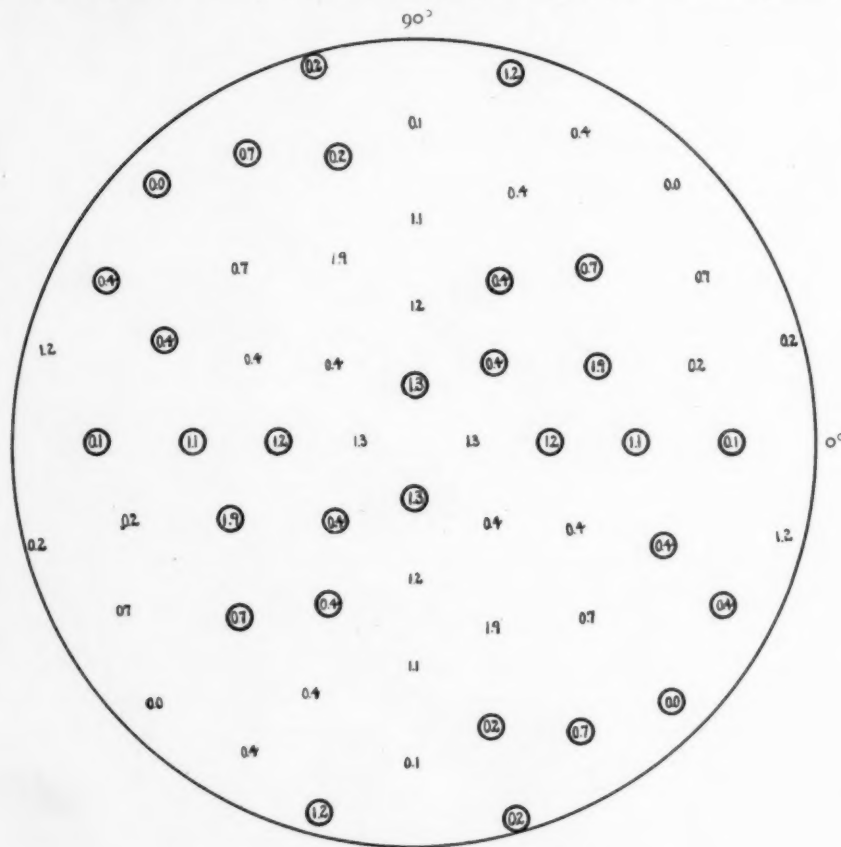


FIG. 5.—Astigmatic Errors of the 40-inch Objective

inclosed in circles. A glance reveals the distribution of the deficient and excessive values. Considering the objective as a whole, there is no well-defined figure showing the direction of the axes of the feeble astigmatism present. The only figure traceable is a double letter *S*, crossed after the fashion of a swastika. Within a radius of 30 cm from the center the axes are more clearly marked. The errors of this kind are all small, only five zones giving errors in the mean values

TABLE III
ASTIGMATIC ERRORS

RADIUS OF ZONE	ϕ	OBJECTIVE ALONE					With CORRECTING LENS		
		1	2	3	4	5	Mean	6	7
mm	15°	mm	mm	mm	mm	mm	mm	mm	mm
490	15°	+0.24	+0.55	+0.34	+0.10	-0.32	+0.18	+1.71	+0.69
480	75	-1.30	-1.79	-1.23	-1.12	-0.76	-0.91	-1.24	-1.24
460	45	-0.49	+0.02	+0.42	-0.01	+0.18	+0.52	+0.02	+1.97
440	60	+0.20	+0.09	+0.69	+0.35	+0.70	+0.55	+0.41	+0.86
420	30	+0.68	+0.74	+0.96	+0.48	+0.72	+0.59	+0.72	+1.47
400	0	+0.10	-0.08	-0.15	-0.15	-0.72	-0.88	-0.14	-0.06
370	15	+0.33	+0.53	+0.52	-0.11	-0.29	-0.42	+0.20	+1.53
340	67.5	+0.18	+0.28	+0.45	+0.31	+0.82	+0.65	+0.41	+0.33
310	45	-1.00	-0.86	-0.59	-0.98	-0.28	-0.01	-0.16	-0.23
280	0	-1.24	-0.89	-1.21	-0.78	-1.29	-1.46	-1.08	-0.54
250	22.5	-2.03	-1.86	-1.68	-1.81	-2.12	-2.67	-1.90	-0.58
230	60	-0.73	-0.28	-0.33	-0.06	-0.54	-0.39	-0.30	-0.17
170	0	-1.45	-2.11	-1.28	-0.31	-0.60	-0.36	-1.15	+0.58
140	45	-0.34	-0.65	-0.04	-0.05	-0.78	+0.58	-0.37	+0.41
70	0	+0.48	+3.40	+0.72	-0.04	+2.16*	+6.44*	+1.34	+1.52

* Poor images.

greater than 1 mm, and four of these are zones of small radii, weak in light-gathering power, and of small divergence.

With the correcting lens in position the astigmatic errors are of about the same magnitude as with the objective alone. They are given in Table III.

The tests described above have been confined to fifteen zones irregularly distributed on the objective, being somewhat crowded at the edge, and the result for each zone rests on but four points. Had I rotated the diaphragm, thereby obtaining additional material for each zone, it is probable that some of the smaller irregularities in the zonal focus-curves would have been eliminated, and T would have

90



A. Foucault.

B. Foucault.

C. Extra-focal.

FIG. 6.—“Focograms” of the 40-inch Objective

been somewhat reduced. The results obtained, however, probably represent the quality of the object-glass as well as a test depending upon a limited number of points can. It might be well to state here that under the best conditions the objective has separated double stars down to its theoretical resolving power.

In order to depict the 40-inch objective as a whole, I have again followed Hartmann, who has recently applied photographically the Foucault knife-edge test to the 80-cm objective at Potsdam, revealing an astonishing amount of detail in the surface, even traces of the epicycloidal motion of the polishing tool. (See the translation of his paper on page 254 of this number.)

I have made several exposures, principally on *Sirius*, introducing the knife-edge from different directions. Two of these images are reproduced in Fig. 6, *A* and *B*. These show the objective in $\frac{1}{40}$ its

natural size. The telescope was west of the pier and directed toward *Sirius*. In *A* the knife-edge was inserted from below, in *B* from the left, the pier side. The arbitrary position angles on the objective used in the zonal work are retained here.

No set of epicycloids is recognizable but there are some minute irregularities of curious form. Most noticeable is the stria crossing the objective in $\phi = 130^\circ$. This, together with the stria at $\phi = 295^\circ$, was seen in a visual knife-edge test. Aside from these striae, most conspicuous are the gap near the edge, corresponding to the depression in the zonal curve at $r = 470 - 480$ mm, and the quadrangular configuration near the center which may perhaps cause the larger astigmatic errors of the small zones. In *B* there are four dark spots caused by bits of frost on the object-glass. *A* was taken under much better conditions of seeing than *B* and consequently shows greater contrast. It is interesting to notice the difference in the illumination on certain irregularities in *A* and *B*, which depends on the direction of insertion of the knife-edge. Aside from the irregularities noted, the objective is very uniform.

The irregularities of surface or of density in the glass are perceived because they give variations from the mean focal plane of the objective. These variations should cause non-uniformity in the distribution of light in the extra-focal star image, and here the pattern should be similar to the irregularities of the objective. Photographs which I have made of the extra-focal star image, Fig. 6, *C*, confirm this. Practically all of the irregularities shown in *A* and *B* are traceable in *C*, although, naturally, there is not the sharpness shown in the knife-edge plates. *A* and *B* show the causes of the effects vaguely apparent in *C*.

COLOR-CURVE OF FORTY-INCH OBJECTIVE

A re-examination of the color-curve of the objective was a part of my programme, and for this purpose I assembled a small spectrograph and made tests by means of extra-focal star spectra. The screen before the objective, shown in Fig. 7, had apertures measuring 6×16 cm, on three different zones at radii $r = 170, 310$, and 450 mm. I am indebted to Mr. Wallace for the preparation of plates for the tests. They were bathed in an aqueous ammoniacal solution of pinacyanol + pinaverdol + homocol, as described in his recent paper on

"Orthochromatism by Bathing."¹ For this plate he has adopted the name "pan-iso." With them I obtained spectra measurable from H_{α} to H_{θ} when working outside of the focus. A pair of these spectra

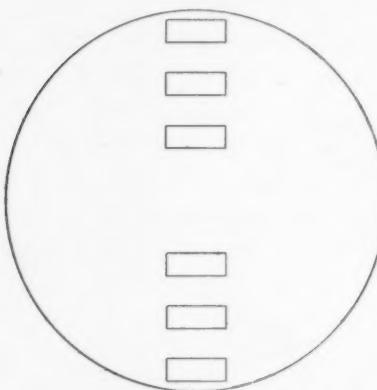


FIG. 7.—Diaphragm for Color-Curve Spectra.

influence of temperature is clearly a mean between the dots and the crosses. This color-curve is practically identical with that by Ellerman² and with an unpublished curve by Frost determined by the older method of strictures in stellar spectra.

As the color-curve was determined for three different zones, there is material for a meager test for zonal errors in monochromatic light. Zones $r=450$ mm and $r=310$ mm give results in close agreement. In the visual portion of the spectrum the latter gives results in excess of the former by a few tenths of a millimeter. This is contrary to the

exposed on *Vega* is shown in Fig. 8. Three pairs of plates were measured to determine the color-curve of the objective alone. The results are given in Table IV. As the recorded temperatures for the three pairs of plates varied but slightly, the results are directly comparable. I have plotted the mean results for the three plates in Fig. 9, where I have indicated data from plate 1 with circles, from plate 2 with dots, and from plate 3 with crosses. The indicated; the open circles are a

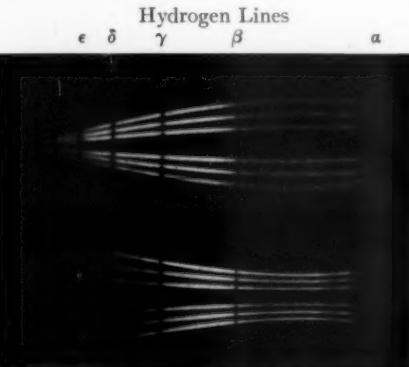


FIG. 8.—Spectra for the Determination of the Color-Curve (*Vega*).

¹ *Astrophysical Journal*, 26, 316, 1907.

² *Ibid.*, 10, 94, 1899.

FORTY-INCH YERKES OBJECTIVE

251

TABLE IV
COLOR-CURVE OF FORTY-INCH OBJECTIVE

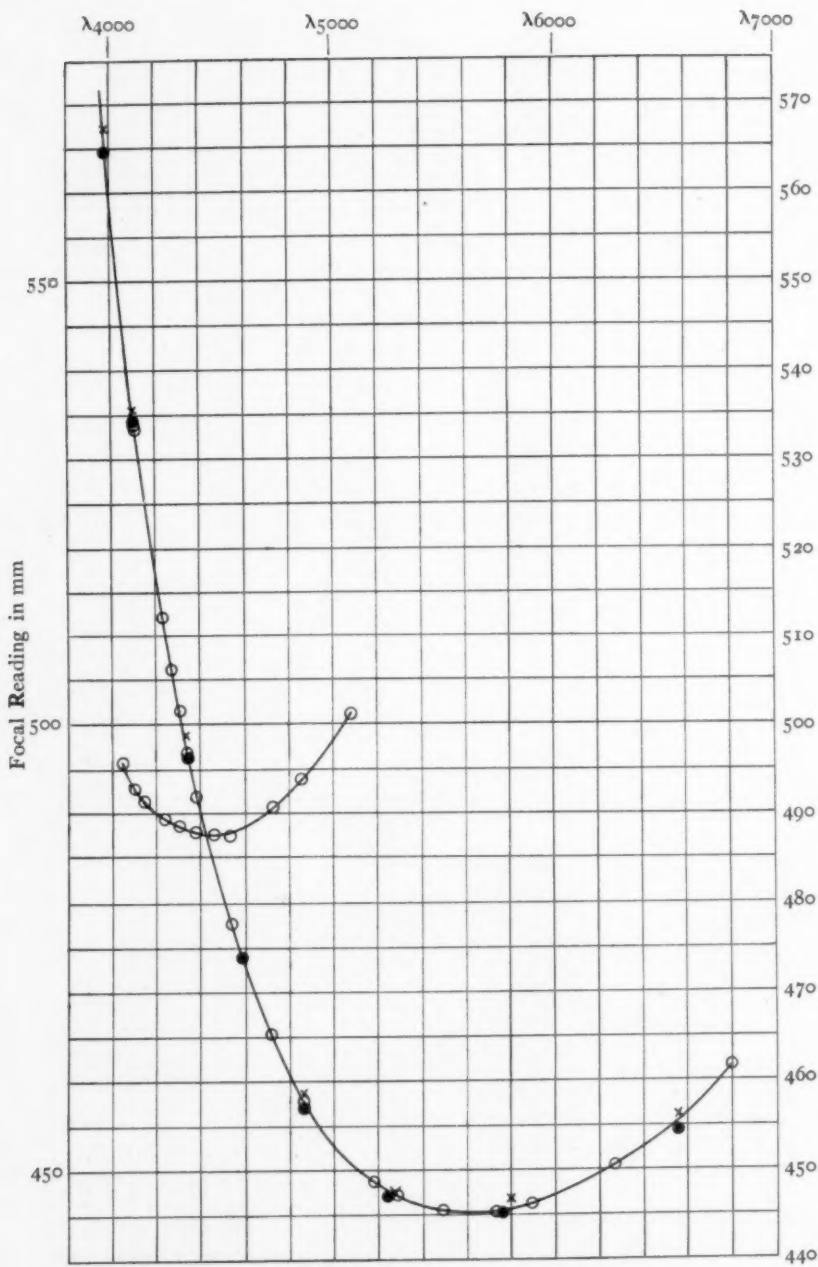


FIG. 9.—Color-Curve of the 40-inch Objective

results from the zonal investigation, where plates 4 and 5 give about 0.2 mm in the opposite direction. The quantities are small, however, so that this disagreement is not severe. Zone $r = 170$ mm is between three and four millimeters shorter than the outer zones and this is in agreement with the zonal results. In the photographic regions the results from zone $r = 450$ mm are larger than those for $r = 310$ mm, and the differences between results for $r = 450$ mm and $r = 170$ mm have increased. In the red regions zone $r = 450$ mm gives smaller readings than $r = 310$ mm. These are the expected consequences of the chromatic difference of spherical aberration.

In Fig. 9 I have also plotted the color-curve obtained with the spectrographic correcting lens in position using the mean values. The data are given in Table V. Zone $r = 450$ mm gives longer focal lengths than $r = 310$ mm by about 1.5 mm and longer than $r = 170$ mm by about 9 mm, differences slightly greater than are shown in the zonal work.

TABLE V
COLOR-CURVE WITH CORRECTING LENS

A	FOCAL READINGS IN MILLIMETERS			
	450	310	170	Mean
5080.....	504.82	502.63	495.89	501.11
4861.....	497.53	495.89	488.08	493.83
4730.....	494.56	492.61	484.82	490.66
4535.....	491.41	489.39	481.48	487.43
4460.....	491.14	489.67	481.79	487.53
4383.....	491.19	489.74	481.88	487.60
4340.....	491.31	489.58	482.36	487.75
4308.....	491.76	490.41	483.17	488.45
4272.....	492.14	490.32	483.17	488.54
4227.....	492.99	491.10	483.61	489.23
4200.....	492.95	491.46	484.52	489.64
4140.....	494.34	493.23	486.38	491.32
4102.....	495.82	494.22	487.87	492.64
4046.....	499.15	497.47	490.81	495.81

I have presented somewhat in detail the results of the investigation of the 40-inch objective and I close by reiterating Professor Hartmann's wish that data might be published for every objective in active use.

I wish to express my indebtedness to Professor Frost for advice concerning the investigations; to Professor Slocum for measuring certain of the plates, and to Mr. Sullivan for assistance at the telescope.

YERKES OBSERVATORY

March 2, 1908

AN IMPROVEMENT OF THE FOUCAULT KNIFE-EDGE TEST IN THE INVESTIGATION OF TELE- SCOPE OBJECTIVES¹

BY J. HARTMANN

Until very recently matters were in an unsatisfactory state in regard to judging of the relative quality of the large objectives and mirrors used in astronomical observations, inasmuch as all data as to individual instruments rested for the most part on the subjective impressions of a few observers. A uniform measure of the quality of the different refractors and reflectors was wholly lacking. The method of extra-focal measurements² which I developed in 1899 first made possible a numerical determination of the so-called zonal errors and of the astigmatism, and this method has since then yielded a series of interesting conclusions as to different instruments. It has been used in several optical works for testing and perfecting their output, and has also served for correcting the principal error of the 80-cm objective of the astrophysical observatory at Potsdam. To recall it briefly, the procedure consists in isolating certain of the parallel rays from the cylinder of rays entering the objective, when it is pointed at a star, by a diaphragm perforated with holes and placed in front of the objective; the course of these rays is determined by obtaining the points of their intersection with two parallel planes.

In continuing the application of this method to the investigation of objectives as well as of complete spectroscopic apparatus, I frequently noticed that closely adjacent points of an optical system often indicated a quite decidedly different path of the rays, whence it was necessary to conclude that these systems occasionally fail to produce as regular a refraction as is ordinarily assumed. In addition to the extra-focal method, which gives the course of the rays for any desired points on an objective, though necessarily limited in number, it seemed to me desirable to have a second method of testing which

¹ Translated from *Sitzungsberichte der K. Preussischen Akademie der Wissenschaften*, Session of December 19, 1907.

² *Zeitschrift für Instrumentenkunde*, 20, 51, 1900; 24, 3, 1904.

should furnish a general view of the optical uniformity of the whole cylinder of rays transmitted by the objective, and thus permit the immediate recognition of the different parts of the optical system which cause an incorrect refraction.

It was clear to me from the start that such a process for testing could be obtained by a suitable application of the well-known "Schlieren" method proposed by Toepler in 1864; or better, by the method introduced six years earlier by Foucault, which is a special case of the Toepler experiment. In the so-called Foucault knife-edge test, the knife-edge is moved in from one side of the focal image of a terrestrial point-source, and the eye, placed close behind the focus, observes directly how the rays are thus cut off. If the objective is free from error, and therefore unites all of the rays coming from the source into a point image, then the eye held at a slight distance behind this image beholds the whole surface of the objective illuminated uniformly, and this light disappears uniformly over the whole surface as soon as the point image is concealed by the knife. But if there are some places in the objective of different refraction, the rays coming from these places will either be cut off before the principal image is concealed by the knife, and they will therefore appear as dark places on the luminous surface of the objective; or this irregularly refracted beam will not be cut off until after the principal image is concealed, and in this case the portions of the objective in question will betray their presence as bright spots on the surface of the objective already darkened by the knife.

This method of Foucault has been introduced in many optical works, and constitutes the principal means for the more accurate testing of objectives and mirrors. The method has, however, hitherto never been employed for testing on the sky an already mounted astronomical refractor; probably for the reason that various difficulties arise in its application.

These difficulties consist, on the one hand, in the impossibility of using a monochromatic source of light in observations on the sky, and, on the other hand, in the constant motion of the image due to the unsteadiness of the air. These two causes make it impossible to obtain a sharp occultation of a point focal image in the astronomical application of Foucault's method. It is nevertheless possible, as I

have found, to perceive in this way at least the larger zonal errors of an objective and this without further apparatus. It is sufficient for this purpose to place a strip of paper having a sharp edge, or a piece of tinfoil, over the opening of the adapter after the eyepiece has been removed, and then to move the paper so that its edge falls in the plane of the image, and thereafter to bring the image of a bright star on the edge by means of the slow motions. As long as this image is not reached by the edge, an eye close to the edge will see the whole objective uniformly bright in the cone of rays. But if the cone of rays is partly cut off by the edge, then brighter and darker places will appear on the objective, which give it a peculiar appearance as if seen in relief. The figure is intended to represent schematically an

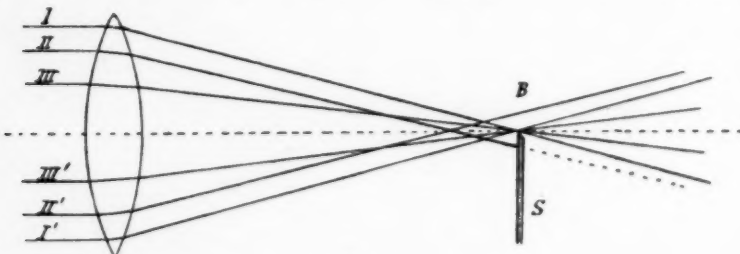


FIG. I

objective, the greater portion of the surface of which unites in the focus B , the rays passing through the outer zone I as well as the central portion III, while there lies between these a zone II of shorter focal length. If the knife-edge S , which is brought up to the point B from below, has not quite reached this, then only the ray II of those shown in the figure will be cut off, and the eye will therefore see the surface II, which is of too short focus, as dark on a bright background on the side of the objective away from the knife-edge. If the knife-edge is moved farther on, so that it catches the rays passing through the point B , then only the ray II', which similarly comes from the zone of too short focus, reaches the eye of the observer. This zone will therefore appear bright on a dark ground on the side of the objective toward the knife (lower side in the figure). It follows from this that such a zone of too short focus presents exactly the same appearance which would be given by the slope toward the edge of the objective (hence outward) of an annular elevation on the ob-

jective, if this was given a very oblique illumination from the side from which the knife-edge was brought up. A similar consideration shows that a zone of too great focal length will be represented as the inner slope of an annular ridge, or as the slope, facing the center of the objective, of a depression.

In the experiments I made in this manner on the 80-cm objective of the Potsdam refractor, I could recognize an apparent crater in diameter about equal to one-third of the diameter of the objective, and this fully confirmed what I had previously determined numerically by the extra-focal measures: the objective had in the zone $r=12$ cm a focal length too short by about 2 mm, but farther in, at $r=8$ cm, a too great focal length. A closer observation of the figure of the objective was hindered by the difficulties above mentioned, the image being very strongly colored by the secondary spectrum and very variable on account of the unsteadiness of the air. However, since there appeared to be further fine details on the surface of the objective which could not be determined with certainty on account of the continuous motion, the idea occurred to me of overcoming the difficulties mentioned by replacing the eye by a camera, the objective of which should throw upon the photographic plate a sharp image of the objective to be investigated. The motion of the stellar image was thus rendered entirely harmless, causing only a variable intensity in the illumination of the separate parts of the image, and thus contributing to a uniform effect in the formation of the image of the whole surface of the objective. The error due to color loses its disturbing effect because the photographic plate is not sensitive for the red and yellow rays, while the photographically active rays of shorter wave-length are well united by the objective. The knife-edge was in this case attached closely in front of the objective of the camera screwed on to the adapter at the eyepiece of the refractor. I will designate these pictures, in which the structure of the focus is photographically recorded, as "focographic" plates.

The result of my plates made in this way was quite astonishing. They showed a wealth of detail in the figure of the objective which was previously entirely unknown. This is shown in the reproduction of one of these "focograms" better than in words. Fig. 2 is the photographic image of the 80-cm objective in one-tenth its natural

size. We first recognize the ring lying at the middle of the lens, which gives to the picture a resemblance to one of the craters of the moon when illuminated from the left. This circular wall is the image of the above-mentioned zonal error. Next we recognize on the whole surface a sort of network of circles crossing each other, doubtless to be regarded as an effect of the epicyclic motion of the polishing tool. The brighter and darker spots that are irregularly distributed would probably be caused by slight irregularities in the



FIG. 2

mass of the glass. This is particularly true of the numerous thread-like streaks which are seen in the right-hand lower half of the picture; these are the so-called waves or threads in the substance of the glass. Finally the few bubbles and small "stones" are also represented as sharply defined white points. We can readily see that the threads and bubbles exert no disturbing effect on the density of the glass in their neighborhood, so that they do not injure the quality of the image.

I would here remark particularly that the 80-cm objective, while not indeed perfect, is still very good and gives quite sharp images.

If the optician should so figure it that all the irregularities here represented should be decidedly reduced, a process rendered much easier by these "focograms," then without doubt the highest perfection possible for this instrument would be reached. I will further add that investigations which I have made on other objectives have shown other phenomena which are in general similar. This focographic procedure is admirably adapted for the investigation of a spectrograph, since it instantly gives a clear picture of the effectiveness of the whole optical system. I shall report on this more thoroughly in another place.

POTSDAM

THE SPECTRUM NEAR THE POLES OF AN IRON ARC

BY W. GEOFFREY DUFFIELD

Liveing and Dewar¹ in 1888 chronicled the occurrence of spark lines in the arc spectrum of magnesium. In 1903 Hartmann and Eberhard² found similar lines for silicon, zinc, and cadmium, and in the same year Hartmann³ published an account of their behavior in the magnesium arc. Barnes⁴ has also worked on this subject, investigating the effect of dielectric density on the intensity of the magnesium line. The most recent publication is that of Fowler⁵ who describes the appearance in the iron arc of lines which are strongest at the tips of the poles and diminish in intensity as they approach the center. Though visible upon both poles, they are stronger at the positive pole. Fowler investigated the region F to C and pointed out the identity of these lines with the enhanced lines of iron and with those lines that are weakened in sun-spots. Photographs showing the same phenomenon (Figs. 1 and 2, Plate XVIII) have also been obtained by the writer with the large 21½-ft. Rowland grating of the Physical Laboratory of the Manchester University, and in view of the application of this investigation to solar phenomena (the extension of the sun-spot spectrum into the ultra-violet having recently been accomplished at Kodaikanal Solar Physics Observatory) and to the resolution of spectral lines into series, the lines presenting this appearance have been identified, and a list is given below for the region $\lambda = 2350$ to $\lambda = 3500$.

The photographs were obtained by focusing a vertical image of the iron arc upon the vertical slit of the spectroscope, the length of the arc being so adjusted that the tip of each pole was just included upon the slit. The spectrum employed was of the first order where the dispersion is 0.4 mm per Ångström unit, and where the astigmatism

¹ *Proc. Roy. Soc.*, **44**, 241, 1888.

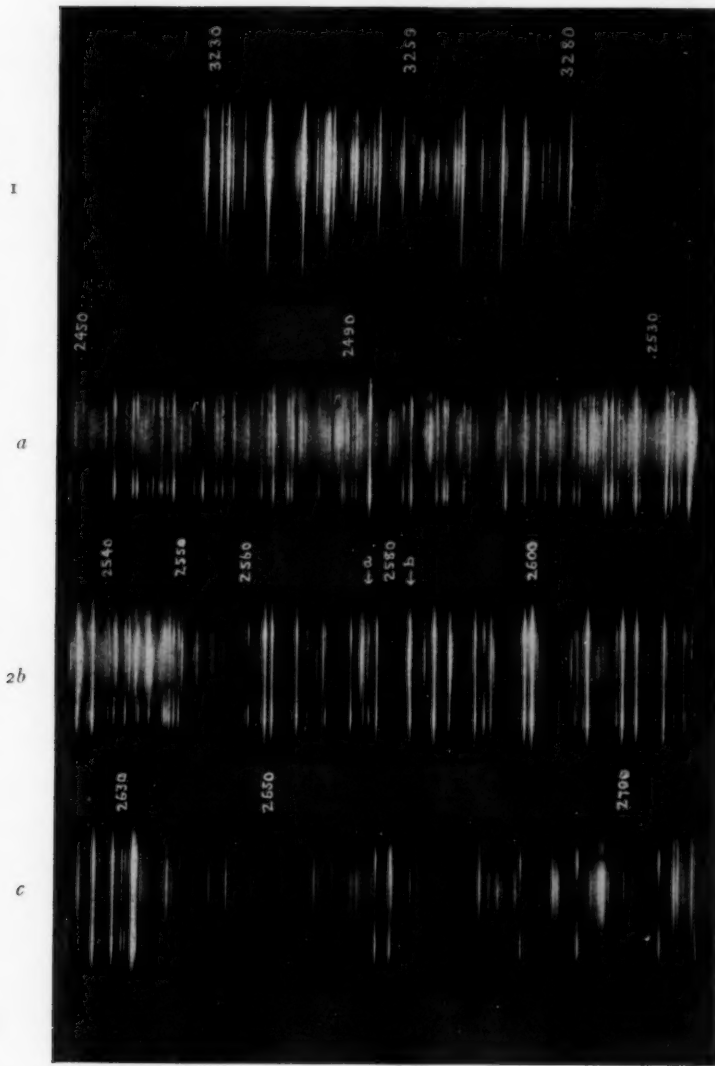
² *Astrophysical Journal*, **17**, 229, 1903.

³ *Ibid.*, 270, 1903.

⁴ *Ibid.*, 21, 74, 1905.

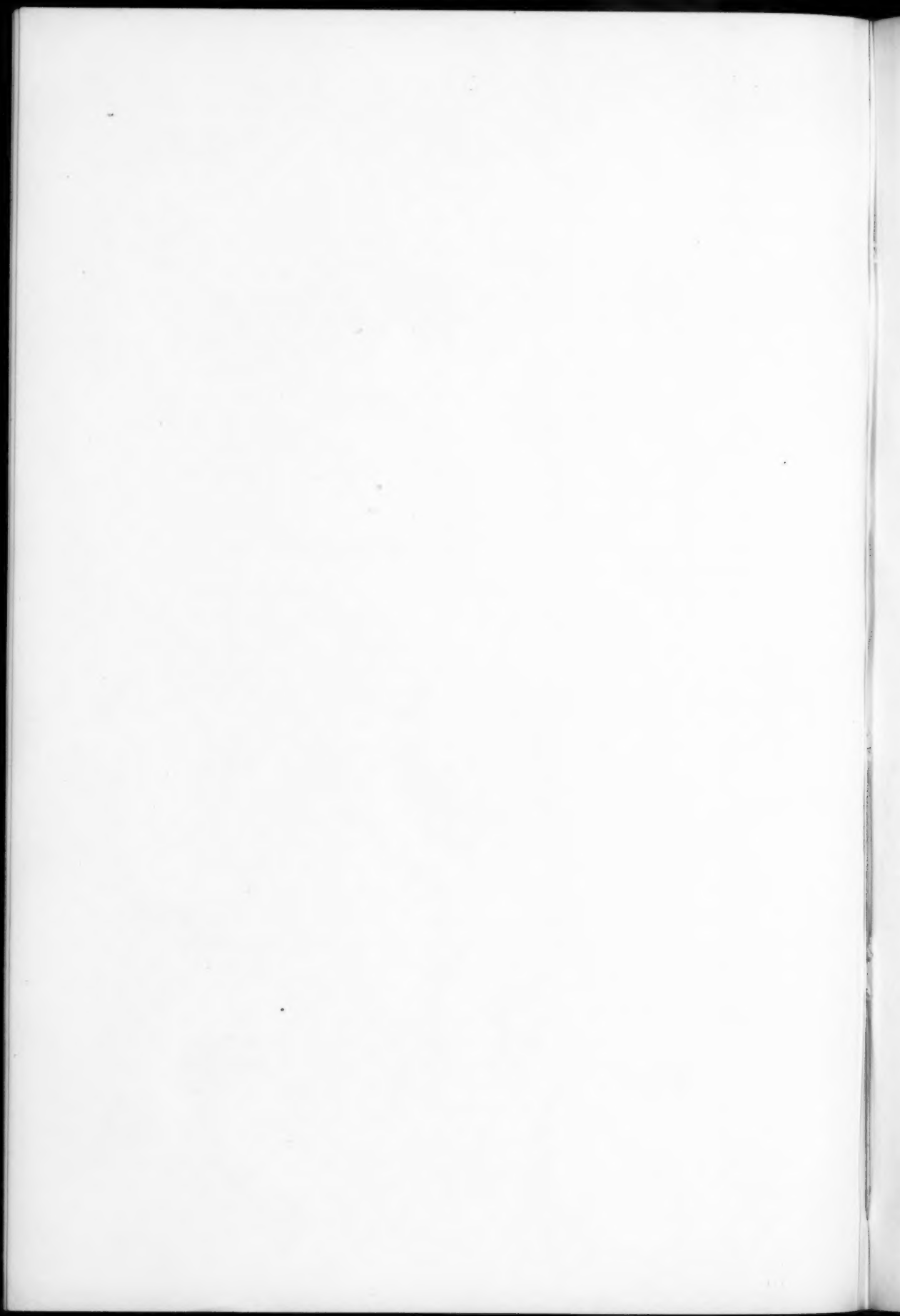
⁵ *Monthly Notices, Royal Astronomical Society*, **67**, 154, 1907.

PLATE XVIII



POLAR LINES IN THE IRON ARC

1. Pair of Polar Lines at λ 3259.
2. *a. b. c.* Polar Lines in the Ultra-violet Region.



is not sufficiently great to mask the phenomenon. The arc was at first fed from the city mains with continuous current, 40 volts being used across the terminals and 12 amperes being recorded by an ammeter in series with the arc.

The photographs obtained differ from those of Fowler in that the lines which appear most strongly at the tips are usually of the same intensity on the two poles. This is well shown by the pair at 3259 (Fig. 1), and by many lines in Fig. 2.

Identification of the lines.—For the region 2400 to 2550 Ångström units, direct measurements were made from the plates, the standards used being those lines for which there was good agreement between the measurements of Kayser and Runge for the arc and those of Exner and Haschek for the spark. For lines of wave-lengths less than $\lambda = 2400$ and greater than $\lambda = 2550$, Kayser's atlas of the iron arc spectrum was employed, but measurements were made whenever it seemed necessary.

Table I contains lists of the arc (K. and R.) and spark (E. and H.) lines whose wave-lengths approximate most closely to those of the lines appearing near the poles of the arc, together with measurements of the wave-lengths of the last-named when these were made. Estimates of the intensities of the lines in the three cases are also given, but as these were made by different observers they are not strictly comparable, and too much stress must not be laid upon their relative values. In the Table 1 is the smallest and 10 the greatest intensity.

A more valid comparison of the intensities of the lines appearing on the poles with those of the spark discharge has been made: a spark discharge was obtained by feeding the primary of an induction coil, whose hammer was clamped, with an alternating current (50 volts) and placing a Leyden jar in parallel with the spark-gap in the secondary. The usual form of comparison shutter was used and by its means a spectrum of the spark was compared with the spectrum given by the tips of the poles.

For the ultra-violet region $\lambda = 2350$ to $\lambda = 2631$ very little difference was found between the spark discharge and the arc spectrum, the lines of which were confined almost entirely to the neighborhood of the poles, the relative intensities of the lines being almost identical in this region in the two cases. But above $\lambda = 2631$ a marked

difference between the two spectra makes its appearance, the lines of the arc being no longer mainly confined to the poles, but occurring, as in the characteristic arc spectrum, most strongly in the center of the arc. Nevertheless many lines still appear with greatest intensity on the tips of the poles and the comparison spectrum shows that in nearly all cases these correspond to lines in the spark, though not now with such close correspondence between their intensities: some few lines at the poles are without counterpart in the spark (e. g., 3076.54, 3078.79, 3132.10), and others which are sharp at the poles are fuzzy in the spark. On the other hand, to all lines occurring in the spark there are corresponding lines in the arc spectrum (with generally some small differences in their wave-lengths in the two cases) either at the center or at the poles of the arc. The conclusion reached is that both the wave-lengths of the lines occurring at the tips of the poles and their intensities point to their being more closely related to the spark than to the arc spectrum; but, since the relative intensities of the lines in the spark depend upon the capacity and self-inductance in the circuit,¹ too much stress is not placed upon the origin of the lines suggested in this way.

In view of these facts it is the writer's conviction that the term "spark" line is misleading when applied to lines which occur in what is to all intents a normal iron arc. More correctly they are lines which occur under conditions which may obtain both in the arc and in the electric spark, the property they have in common in the two cases being their most pronounced occurrence in the neighborhood of the poles. I suggest "polar lines" as a term less ambiguous than that of "spark lines." For those lines occurring most strongly in the center of either the arc or the spark, the term "median lines" seems suitable.

None of the ten photographs obtained in 1905 fails to show this phenomenon. It was suggested as a possible explanation of the appearance of these lines in the arc spectrum that a superinduced alternating current might have disturbed the continuous current supplied by the city mains, and have produced a weak spark discharge. The same effect was, however, obtained upon each of four additional exposures made when the current was taken from the storage batteries

¹ G. A. Hemsalech, *Journal de physique*, 9, 437, 1900; G. E. Hale, *Astrophysical Journal*, 15, 132, 1902; W. B. Anderson, *ibid.*, 24, 221, 1906.

in the building. It should also be added that the exposure was not begun until the arc had been struck, and that it continued to burn steadily until the shutter was closed. In the photographs of the spark used for comparison the positive bands of nitrogen at $\lambda 3371$ and $\lambda 3158$ appear at the tips of the poles.

The effects of temperature, density, etc.—Various explanations have been proposed to account for the loss of luminosity of the polar lines as they proceed toward the center of the arc. Apart from the appearance of these lines, differences in the spectra¹ emitted by different parts of the arc have frequently been recorded and have been variously ascribed to differences in density, temperature, and potential gradient. Temperature does not seem able to explain the whole phenomenon, since the occurrence of these lines showing scarcely any difference in their intensity at the two poles (in many cases no difference is discernible) is not in accord with this hypothesis. Hartmann has found other grounds for rejecting it. Liveing and Dewar obtained the lines in the case of magnesium when the electrodes were surrounded by air, ammonia, steam, carbon dioxide, chlorine, and other gases, hence the inference is that the lines are not due to chemical interaction between the metal and the surrounding gas.

The cross-section of the arc is smallest in the neighborhood of the poles, hence it is natural to expect that a larger amount of light-energy will be admitted through the parallel jaws of a slit where the image of the poles falls upon it than where the center of the arc is focused. This may partly explain the decrease in the intensity of the lines as they approach the center on the supposition that the vapor producing them is homogeneously distributed throughout the arc, though it adds to the difficulty of explaining the characteristic formation of the arc or median lines in the center. Homogeneous distribution does not exist, however, and near the poles the greater velocity of the particles should effect a reduction in the number of particles present in unit volume and a consequent diminution of the photographic effect. The greater width of the lines near the poles may be effected by the greater velocity of the particles near them (if the arc and the spark are in this

¹ J. N. Lockyer, *Phil. Trans.*, 163, 253, 1873; Thomas, *Comptes Rendus*, 119, 728, 1894, etc.; H. Kayser, *Handbuch der Spectroscopie*, I, 165; H. Crew, *Astrophysical Journal*, 20, 274, 1904

respect similar), which would render more obvious any line-of-sight motion they might possess after collisions.

The density and pressure are not determinate in an electric arc, and though it is doubtful whether either is constant throughout the arc, this condition is required to explain the fact that there is no observed curvature¹ of the spectral lines as they proceed from the poles toward the center of the arc. Differences frequently exist between the wave-lengths of lines occurring near the poles and those occurring in the center, and these discrepancies are illustrated by the pair at 2563 whose members are at the poles 0.95, and in the center 0.88 Ångström units apart (K. and R.), by the pair at 3259 which are at the poles 0.27, and in the center 0.65 Ångström units apart (K. and R.), and by the polar lines near 2490 which are on the violet edges of absorption lines in the center of the arc. The polar line marked *a* on the diagram at 2576.89 is a typical example of this, as it is on the edge of the line 2576.76 which appears only as a median line. The line marked *b* at 2582.62 is of a similar nature. Though the real correspondence of these lines is not established, the above evidence suggests a pressure or density displacement, but since the lines are invariable in wave-length for the ranges over which they occur, the influence of these physical conditions is doubtfully capable of explaining the displacements of the lines, though the increased width near the poles is quite possibly due to such cases.

On the other hand, the electrical conditions appear to determine the character of the explosion which takes place at the poles; upon the conditions of the disruption may depend the nature of the particle shot out and the type of vibration it possesses. According to Walter² who studied the "arc lines in spark spectra" the essential difference between the polar and median lines consists in the former being due to charged and the latter to uncharged particles—certainly the gradual appearance of lines in the center of the spark after the gradual disappearance of lines at the poles is suggestive of some action of this sort; a more radical change in the constitution of the particle is not out of the question.

Resolution of the lines into series.—The table which accompanies

¹ A difference in wave-length corresponding to a difference in pressure of two or three atmospheres should be capable of discovery.

² *Annalen der Physik*, 21, 223, 1906.

this paper will, it is hoped, assist in the resolution of the complex iron spectrum into series of lines; in it are included all lines observed with decreasing intensities as they proceed from the poles to the center of the arc. There is, however, a large range in their luminosity gradients, and a detailed study of these might further assist the resolution of the iron spectrum into series; but for this investigation photographic intensities are scarcely sufficiently reliable to justify the expenditure of the necessary time.

The median lines.—The character of the spectrum due to the center of the arc is of considerable interest; whereas the lines appearing near the poles are sharp and clearly defined, those in the center are very often diffuse and nebulous, this being specially noticeable where the polar lines are very numerous, e. g., in the extreme ultraviolet. Where they are less frequent the median lines are sharper, cf. the part of the spectrum near $\lambda 3260$ (Fig. 1). The nebulosity was thought at first to be due to a continuous spectrum produced by the poles of the arc, but the careful adjustment of the image of the arc on the slit precludes this explanation. It also sometimes happens that when a polar line occurs close to a median line, the polar line appears to gain in intensity at the expense of the median line. The pair at $\lambda 3259$ affords an example of this; it is shown in Fig. 1 on the accompanying plate. The members of this pair of polar lines (intensity 4) are 0.30 Å. U. apart, and, though Kayser chronicles a pair of lines (intensity 1) in the normal arc about twice this distance apart (0.65 Å.U.), of which one line is identical with the red member of the polar pair, the violet member of the median pair ($\lambda 3258.50$) is generally, though not invariably, much weakened when the polar lines are pronounced; it is absent from the photograph reproduced in Fig. 1. On other plates on which the polar pair is less strong, this violet median line is sometimes the strongest of the three. In Fig. 1 the absence of the median lines is possibly due to the energy of their vibration having been transferred to the particles producing the narrower pair near the poles.

The pair $\lambda 2562.59, 2563.54$ affords another and similar example of the above phenomenon, and the table includes more complete evidence of the changes in relative intensity between the median and polar lines.

I take this opportunity of expressing my gratitude to Professor Schuster for having placed the necessary apparatus at my disposal.

TABLE I
POLAR LINES IN THE ARC SPECTRUM OF IRON

Arc (K. and R.)	Arc Intensity*	Spark (E. and H.)	Spark Intensity*	Intensity at Poles*	S = Resembles Spark A = Resembles Arc Spectrum	Measurements of Polar Lines
2360.06	8	2360.08	5		S	In this part of the spectrum the intensities of the polar lines are difficult to estimate with the necessary accuracy. Direct comparison with a spark spectrum shows that the two are very similar
60.37	8	60.42	5			
64.88	10	64.90	7			
68.66	8	68.69	8			
75.30	8	75.30	6			
79.38	8	79.36	7			
80.82	6	80.86	5			
82.15	10	82.13	9			
83.24	8	83.17	2			
90.03	4	90.04	1			
95.62	10	95.73	7			
99.31	10	99.31	8			
2405.02	10	2404.98	7			
06.72	10	06.73	6		S	
10.56	10	10.59	8	6	S	
11.16	10	11.15	7	6	S	
13.37	10	13.36	8	6	S	
24.22	8	24.18	7	4		
30.16	6	30.18	7	4		
32.34	4	32.30	6	2	A	
32.97	2	32.92	6	1	A	
34.86	4	(34.70)	5	4	A	34.86
35.04	6	34.98	5	4		
39.36	6	39.35	6	6		
44.58	6	44.57	6	5		
45.68	4	45.67	4	4		
(49.93)	1	50.28	4	6	S	50.24
58.78	8	58.80	6	7		
61.28	8	61.36	5	6	S	61.35
61.89	4	61.90	5	5		
64.09	1	64.10	4	2		
66.02	2	66.00	4	1	A	
66.81	6	66.87	4	3	S	66.86
70.78	4	70.73	4	2	S	70.73
74.88	8	74.82	3	1	S	74.85
80.25	6	80.22	5	1		
81.11	1	81.11	3	5	S	81.12
82.16	4	82.18	4	5		(Standard)
....		82.78	4	4	S	82.78
88.23	10	88.23	2	3	S	82.22
89.63	4	89.52	3	1		89.59
90.01	4	89.92	5	1†	A	90.04†
90.98	6	90.91	3	1†	A	91.04†
91.50	6	91.47	4	1†	A	91.52†
93.34	10	93.31	8	10		93.29
98.96	10	98.95	7	7		99.00
2502.53	8	2502.49	4	3	S	02.49
03.50	8	03.39	4	2	S	03.41

*Maximum Intensity = 10.

†Each of these three lines is on the red edge of an absorption line in the arc spectrum.

TABLE I—Continued

Arc (K. and R.)	Arc Intensity	Spark (E. and H.)	Spark Intensity	Intensity at Poles	S—Resembles Spark A—Resembles Arc Spectrum	Measurements of Polar Lines
(2503.89)	2	2503.97	5	3	S	03.98
06.98	6	07.11	1	4		07.06
11.84	4	11.85	7	7	S	(Standard)
(19.30)	4	19.14	5	5	S	19.15
25.48	6	25.50	7	7		
26.30	8	26.48	6	6		26.39
29.65	4	29.59	6	6	S	29.59
(33.86)	10	33.71	7	6	S	33.74
34.52	4	34.50	6	6		34.50
35.67	6	35.59	5	3	S	35.60
36.92	8	36.95	5	6		36.94
38.98	{ 10	{ 38.95	5	8		38.94
....	{ 10	{ 39.10	4	9	S	39.06
(40.90)	4	40.72	5	1	S	40.75
41.18	6	41.20	5	4		41.19
(42.20)	8	41.91	5	5	S	41.91
42.85	1		2	A	42.80
43.47	4	43.49	5	7		43.45
(44.83)	8	45.05	3	2	S	45.04 ? Cu
(45.95)	2	45.32	3	4	S	45.30
(46.26)	8	46.80	5	4	S	46.75
(47.06)	8	47.43	4	3	S	47.41
(48.17)	2	48.42	3	1	S	48.37
48.76	6	48.73	3	2		48.78
....		49.20	3	3	S	49.17
49.63	8	49.60	4	5		49.51
50.07	2	(50.20)	5	5	A	50.10
50.75	2	(50.87)	5	5	A	50.75
55.19	3	55.12	3	1	S	55.13
55.59	4	55.54	3	1	S	55.51
(57.42)	1	57.00	3	3	S	57.56
59.91	2	59.84	3	2*	A	59.91
60.43	4	60.39	4	4	S	60.36
(62.35)	4	62.16	3	2	S	62.16
62.63	10	62.59	6	8*	S	
63.51	10	63.54	5	8*	S	
66.99	8	67.01	4	7	A	
74.43	6	74.46	5	6		
76.20	6	76.18	1	3		
(76.76)	8	76.89	5	4†	S	
78.01	10	77.98	5	7		
82.50	10	82.62	7	8‡	S	
85.93	10	85.96	8	9		
88.11	10	88.05	5	4	S	

* At the poles the distance apart of these two lines is 0.05 Å. U. indicating that they approach the spark, rather than the arc.

† Marked *a* on photograph.

‡ This line (marked *b* on the photograph) is apparently reversed in the ordinary arc spectrum, but in this photograph is seen to be composed of two lines originating in different parts of the arc.

TABLE I—Continued

Arc (K. and R.)	Arc Intensity	Spark (E. and H.)	Spark Intensity	Intensity at Poles	S = Resembles Spark A = Resembles Arc Spectrum	Measurements of Polar Lines
2591.65	8	2591.65	6	7		
92.90	4	92.87	6	6		
93.75	6	93.80	4	6		
98.44	10	98.43	9	9		
99.53	10	99.50	10*	10		98.43
(2605.77)	8	2605.40	1	3	S	05.43
(06.92)	4	06.60	4	3	S	06.60
07.16	8	07.17	9	9		(Standard)
09.30	1	09.26	2	1		
11.16	2	11.16	3	3		
11.94	10	11.95	9	10		
13.91	8	13.91	9	9		
17.71	6	17.70	7	10		
21.72	8	21.78	6	6	S	21.77
25.72	10	25.67	5	8*	S	25.66*
.....		25.80	7	8*	S	25.78*
26.52	1	26.60	4	4	S	26.58
28.35	10	28.40	9	8*	S	28.39
29.66	1	29.67	5	5	S	(Standard)
30.13	2	30.16	3	5		30.15
31.07	10	31.14	4	7	S	31.13
31.37	10	31.46	4	7*	S	31.42
31.72	2	31.79	3	5	A	31.71
37.69	1	37.72	4	3		
39.60	1	39.66	3	2		
64.72	8	64.78	7	7		
66.72	4	66.75	7	7	S	
84.86	4	84.84	6	6		
92.71	4	92.68	6	6		
97.58	1	97.52	2	1		
2704.06	6	2704.10	5	6	S	04.07
07.13	1	07.23	3	1	S	07.21
09.13	2	09.14	3	3		(Standard)
11.92	2	11.94	4	5		11.92
12.42	2	12.48	2	2		
14.48	10	14.51	7	9		
16.31	4	16.30	4	5		
24.97	8	24.99	4	6		
27.61	8	27.59	8	7		
30.79	8	30.85	4	5		30.81
37.02	8	37.05	5	7		(Standard)
39.59	10	39.67	10	9		39.64
43.23	10	43.34	8	8	A	43.26
46.54	10	46.58	7	9		46.57
47.03	10	47.08	7	9		
49.42	6	49.40	10	10		
53.37	6	53.32	7	7		
55.77	10	55.82	10	10		55.82
61.83	8	61.88	3	6		

* Two lines occur on the poles, one in the arc and two in the spark.

TABLE I—Continued

Arc (K. and R.)	Arc Intensity	Spark (E. and H.)	Spark Intensity	Intensity at Poles	S = Resembles Spark A = Resembles Arc Spectrum	Measurements of Polar Lines
2767.56	10	2767.62	77	8		
68.52	2	68.50	1	4		
68.98	4	69.03	3	4		
79.34	6	79.40	1	1		
83.75	8	83.81	7	6		
85.11	1	3	A	
93.97	2	94.02	3	1		
99.34	1	99.42	2	1		
.....	..	2831.67	5	5	S	31.67
2835.76	2	35.82	4	1	A	35.74
39.66	1	1	A	39.59
.....	..	39.85	2	1	S	39.87
40.73	2	40.82	3	1	A	40.72
48.13	2	48.15	2	3		48.11
49.67	1	49.70	2	2		49.65
55.75	2	55.77	3	1		
.....	..	2 faint pairs	..	2	S	
58.41	4	58.40	5	1		
71.16	1	71.19	2	1		
72.54	1	72.47	3	3		
73.48	2	73.49	4	2		
77.37	8	77.38	1	1	S	
80.84	6	80.89	3	5		
83.80	6	83.80	3	4		
.....	..	86.02	1	1	S	
.....	..	88.20	1	1	SS	
.....	..	94.90	2	2	S	94.86
.....	..	95.35	2	2	S	95.27
97.33	1	97.37	2	1		97.34
2926.65	8	2926.71	3	6	A	
39.39	4	(39.62)	1	3	A	39.38
44.49	6	44.55	4	6	A	44.49
47.77	8	47.78	3	3		47.74
48.52	6	48.52	1	3		48.51
49.28	6	49.30	2	4	S	
64.30	2	64.25	1	1		
64.72	2	64.76	1	2		
65.14	4	65.17	2	3		
70.60	4	70.64	2	2		
79.44	1	79.48	1	2		79.47
(81.95)	6	82.20	1	1	S	82.18
84.92	8	84.97	6	7		84.95
85.65	6	85.70	4	6		
(97.51)	1	97.45	1	2	S	97.39
.....	..	3000.20	1	2	S	300.16
3002.74	4	02.80	3	5	A	02.75
(62.47)	1	62.33	2	1	S	62.33
76.60	2	2	A	76.54*
77.32	1	77.30	2	2		

* No counterpart in spark comparison spectrum.

TABLE I—Continued

Arc (K. and R.)	Arc Intensity	Spark (E. and H.)	Spark Intensity	Intensity at Poles	S = Resembles Spark A = Resembles Arc Spectrum	Measurements of Polar Lines
(3078.50)			2		78.79*
.....			2		3132.10*
3154.29	1	3154.32	5	4		
77.64	1	77.64	3	4		
86.83	2	86.87	3	5	S	
3213.43	1	3213.45	5	1	A	
(58.50)	1	58.90	3	4†	S	
59.15	1	59.20	3	4†	S	
77.42	1	77.48	3	1		
3323.84	6	3323.83	2	1	S	
(3493.78)	2	3493.63	2	1		

* No counterpart in spark comparison spectrum.

† At the poles the distance apart of these two lines is 0.27 Å. U., indicating that they approach the case of the spark, rather than the arc discharge.

SUMMARY

1. In the arc spectrum of iron, some lines appear strong at the poles, diminishing gradually in intensity toward the center of the arc.
2. They have the general appearance of spark lines, but, to avoid ambiguity, the term "polar" lines is suggested to distinguish those lines occurring most strongly at the poles of the arc or the spark from those occurring most strongly in the center, for which term "median" lines seems suitable.
3. The polar lines are usually found with equal intensities on the two poles, but this is not invariably the case.
4. A list is given of the polar lines between $\lambda 2350$ and $\lambda 3500$ together with the intensities of the nearest "arc" and "spark" lines from the tables of Kayser and Runge and of Exner and Haschek.
5. Direct comparison with the spectrum from a spark discharge shows that between $\lambda 2350$ and $\lambda 2630$ all lines in the spark spectrum have their counterparts in the polar lines in the arc, and that the two spectra show a remarkable resemblance; but with increasing wave-length the arc becomes richer in median lines, some of which now correspond to lines from the spark discharge, and the polar lines decrease in number and intensity.

6. The numbers of polar lines in the arc are:

Between λ 2400 and λ 2500, 34
 λ 2500 and λ 2600, 51
 λ 2600 and λ 2700, 25
 λ 2700 and λ 2800, 27
 λ 2800 and λ 2900, 24
 λ 2900 and λ 3000, 15

Between λ 3000 and λ 3100, 6
 λ 3100 and λ 3200, 4
 λ 3200 and λ 3300, 4
 λ 3300 and λ 3400, 1
 λ 3400 and λ 3500, 1

7. The origin of the polar lines and the bearing of pressure, density, temperature, and potential gradient upon the phenomenon is discussed.

8. The distinctive character of the polar lines should assist in the resolution into series of the iron arc spectrum.

9. The median lines of the arc in the extreme ultra-violet are diffuse and nebulous, the polar lines sharp.

10. Instances are given of median lines losing in intensity in the arc when polar lines appear near them.

PHYSICAL LABORATORIES
MANCHESTER UNIVERSITY, ENGLAND
December 31, 1907

THE SPECTROSCOPIC BINARY *ι ORIONIS*

BY J. S. PLASKETT AND W. E. HARPER

This star (R. A. $5^{\text{h}} 30^{\text{m}} 5$; Decl. $-5^{\circ} 59'$; Photog. Mag. 3.4), announced by Frost and Adams¹ as a spectroscopic binary, was placed under observation here for the determination of its orbit in December 1906. Of the 107 plates used for this purpose, 37 were made between December 11, 1906, and April 1907, with an adapted Brashear universal spectroscope, and the remaining 70 between September 14, 1907, and January 25, 1908, with the new single-prism Ottawa spectrograph. The linear dispersion of the Brashear instrument is 18.6 and of the single-prism spectrograph 30.2 tenth-meters per mm at $H\gamma$. Notwithstanding the greater dispersion of the former instrument more confidence should be placed, in the case of this star, in the results obtained by the latter, for two reasons. With the former instrument, owing to curvature of field of the camera lens, only two lines, He , $\lambda 4471$, and $H\gamma$, $\lambda 4340$, are accurately measurable; while with the latter all the lines, usually five or six from $H\beta$ to $H\epsilon$ inclusive, are available. In the second place, on the broad and diffuse lines of this spectrum, the settings can be more accurately made when photographed with the smaller dispersion.

The spectrum is of the helium type, the lines used for determining the velocity being given in the table below.

LINES IN SPECTRUM OF *ι Orionis*

Elements	Wave-Length
H	4861.527
He	4713.308
He	4471.676
He	4388.100
H	4340.634
H	4102.000
He	4026.352
H	3970.177
Ca	3933.825

The lines $\lambda 4713$, 4388, and 3933 are rarely measurable or even visible on the plates, and consequently they have been used only a few

¹ *Astrophysical Journal*, 18, 386, 1903.

times. The other six lines have nearly always been used in the single-prism plates. Lines of wave-lengths λ 4686, 4543, 4143, and 4089 have been seen on some plates but never used in the velocity determinations. All the lines as stated above are very broad and diffuse, the widths varying between 2 and 4 tenth-meters. They are in many cases so faint as to be only with difficulty distinguished from the adjacent continuous spectrum. The difficulty of setting is further increased by the asymmetry of many of the lines; this asymmetry, combined with their diffuse character, rendering the settings uncertain. A peculiarity about this asymmetry is that all the lines of a spectrum are not necessarily affected in the same way. Some may have the maximum intensity to the red and some to the violet side of the band, while other lines may be nearly uniform. Although in one or two cases some of the lines appear doubled, this is by no means a common characteristic and this apparent doubling should not necessarily be assigned to the presence of a second spectrum, but possibly to some irregular arrangement of the silver grains in the naturally broad, diffuse, and asymmetric lines of the spectrum, or to some physical cause in the star's atmosphere. No evidence of the triple superposed maxima observed by Frost and Adams has been found on any of the plates, but this may possibly be due to the lower dispersion used here.

In consequence of the poor quality of the lines for measurement the radial velocities obtained may, in some cases, be in error to the extent of 15 or 20 km per second. Occasionally in two plates made on the same night there has been a difference of upward of 30 km in the measured velocity. That this difference is in great part due to the character of lines is shown by the fact that measures of the same plates by different observers occasionally differ about 20 km in the velocity. The probable error of a single plate, obtained by the use of the residuals from the final curve of oscillation, is for the Brashear spectroscope plates ± 7.8 km per second, and for the single-prism plates ± 6.6 km per second.

It is only when the range of velocity is large (in this case about 225 km) and where a large number of spectra have been secured, that a satisfactory orbit can be obtained for stars with this type of spectrum. The difficulty, in the present instance, is probably increased by the

high eccentricity of the orbit and consequently abruptly changing form of the velocity-curve, as well as by a probable secondary disturbance giving rise to a secondary curve superposed upon the primary.

The early observations with the Brashear spectroscope indicated a period of about 29 days. When use was made of Frost and Adams' observations of 1903 the period was approximately determined as 29.128 days. When all the observations were brought into one period it was at once seen that plates were required at the maximum and minimum points and along the rapidly descending branch of the curve, 3 or 4 days out of the 29. Cloudy skies at every recurrence of this epoch prevented these being secured during the winter of 1906-7, and it almost seemed that the same bad fortune was to prevail in 1907-8. Although partial success was obtained in October 1907, it was not until January 24 and 25, 1908, that the final observations necessary were secured. The observations of October indicated a period of 29.134 days, but the later plates changed this to 29.136 days. This can hardly be in error more than the thousandth of a day, as it is determined by the coincidence of an observation of Frost and Adams on September 5, 1903, with the rapidly descending branch as finally defined on January 25, 1908, 55 periods distant.

Originally each single measurement was plotted on cross-section paper, but as the number increased, plates taken on the same night (sometimes five in number at critical parts of the curve) were combined and their mean, weighted according to the quality of the plates, was used. When the period had been accurately determined those of nearly the same phase were grouped together and treated in the same way. In thus combining the observations there are only two groups (near apastron, where the change of velocity is slow) in which the difference of phase exceeds a day. The difference in the remainder is less than half a day and in most of these (all around periastron) less than a quarter of a day. This method of grouping prevents confusion and facilitates the drawing of the graph, while the effect of large accidental errors in the velocity values of some of the plates is diminished.

In addition to the 107 observations made at Ottawa, the 6 made at the Yerkes Observatory have been used and the 113 are combined into 27 groups with an average of somewhat over 4 observations each.

The phase, the mean velocity, and the number of measures in each phase are tabulated below.

Most of the measures on the Ottawa plates were made by Mr. Harper, while the grouping and discussion are due to Mr. Plaskett.

PHASES AND VELOCITIES

Phase	Mean Velocity	No. of Plates	Phase	Mean Velocity	No. of Plates
0.65.....	+ 101.3	5	14.53.....	+ 27.4	5
0.82.....	+ 91.0	2	16.67.....	+ 34.7	2
1.60.....	+ 30.8	10	18.44.....	+ 34.3	4
1.85.....	- 21.3	2	19.32.....	+ 41.2	2
2.43.....	- 115.7	10	20.67.....	+ 51.2	5
3.07.....	- 118.2	5	21.55.....	+ 45.3	3
3.44.....	- 92.1	5	22.65.....	+ 57.	1
4.39.....	- 75.7	6	25.30.....	+ 70.0	5
5.33.....	- 47.8	3	26.44.....	+ 79.0	2
6.68.....	- 14.0	2	27.39.....	+ 80.0	4
7.12.....	- 27.3	5	28.16.....	+ 92.1	5
8.89.....	- 2.1	5	28.53.....	+ 105.5	4
11.39.....	+ 15.0	4	28.93.....	+ 104.9	5
13.05.....	+ 9.5	2			

These values are plotted in Fig. 1, where the full line is the velocity-curve corresponding to the elements $e=0.75$, $\omega=110^\circ$, which were finally decided upon as the most probable.

Owing to the considerations previously mentioned, especially that relating to the possibility of a secondary disturbance, a final determination of the elements by the usual methods is out of the question. They only suffice to give preliminary values which must be corrected by a species of trial and error. For this purpose the method developed by Dr. W. F. King¹ has been found very useful as the labor of constructing an ephemeris and drawing the velocity-curve or of changing these to correspond to changes in the elements is reduced to a minimum. Less than half an hour suffices to draw the velocity-curve for any set of elements and consequently the trials of different values can be easily and quickly made.

No simple elliptic orbit will give a velocity-curve agreeing with a smooth curve drawn as closely as possible through the observed points; and we are forced to the conclusion that the differences are due either to errors in the observations or to secondary disturbances in the orbit. The latter seems to be the most likely, for although it is probable

¹ *Astrophysical Journal*, 27, 125, March 1908.

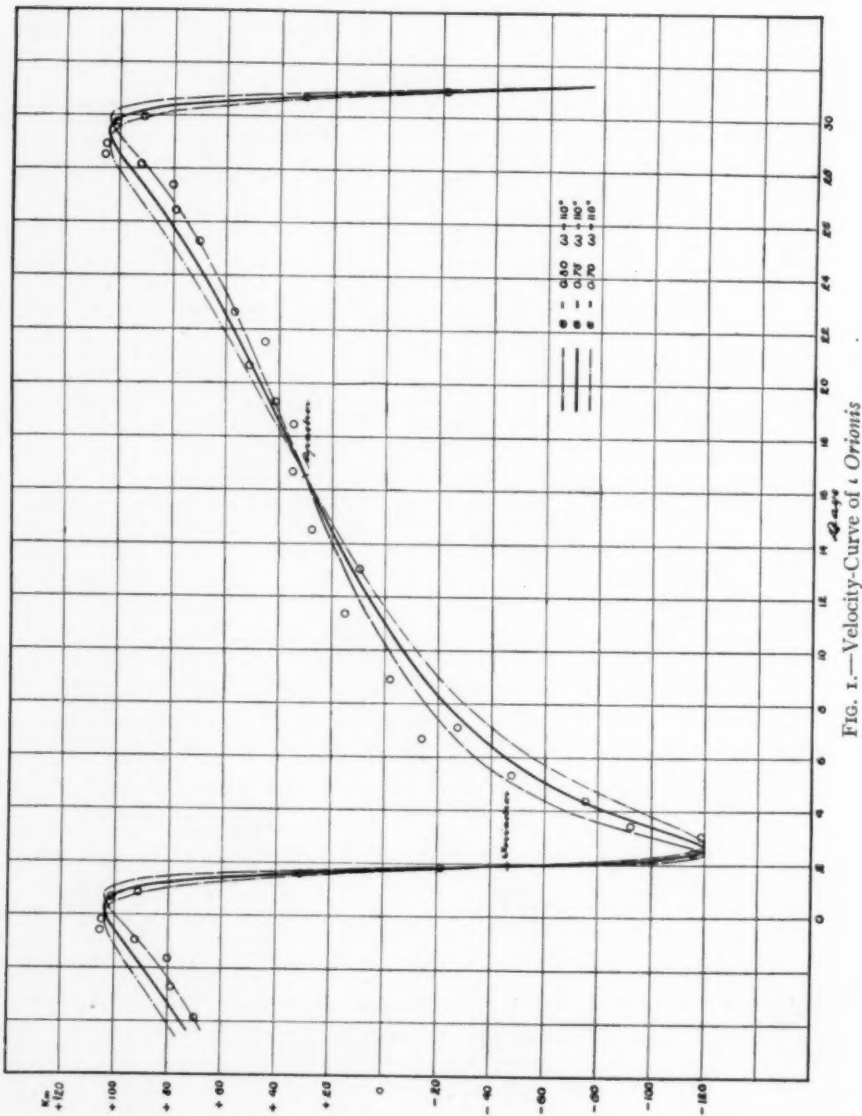


FIG. I.—Velocity-Curve of ι Orionis

enough that two or three observations may be in error to the extent shown by the figure, it is hardly possible that for 10 or 12 days before apastron passage the residuals should be almost wholly negative and for 10 or 12 days after almost wholly positive.

These residuals can be considerably reduced and a curve agreeing fairly well with the observations on the ascending branch may be obtained by increasing the eccentricity to about 0.82. An eccentricity of 0.80 is shown by one of the dotted curves in Fig. 1. The use of an eccentricity of even 0.80 produces much higher residuals on the rapidly descending branch and at the points of maximum and minimum velocity, than an eccentricity of 0.75 in the ascending branch. In the descending branch any errors of observation or even any moderate secondary disturbance would have very little effect on the position or inclination of the curve. It was therefore considered preferable to determine the eccentricity by the inclination of the curve around periastron rather than by agreement around apastron, and it was for this purpose that observations in that phase were so long awaited. A reference to the curves of oscillation, Fig. 1, for $e=0.70$, 0.75, and 0.80 shows that the eccentricity can be determined to within 0.01 by the inclination of the descending branch, and it may be stated that the same criterion may be used to determine the eccentricity, whatever the value of ω . Furthermore, the value of ω is also closely limited by the position of the curve near apastron. A difference of 1° either way would displace the curve too far up or down for the best agreement with the observations.

The above considerations led to the final choice of the elements $e=0.75$, $\omega=110^\circ$ as the most probable, while the question of a secondary curve is left open. The observations, even taking into account their high probable error, indicate the presence of such a curve but do not sufficiently define its position and amplitude to enable any explanation of its cause to be assigned. So far as known to the writer, previously discovered secondary disturbances have been submultiples of the main period, but such is apparently not the case here where the secondary effect persists for 10 or 12 days on each side of apastron, about three-fourths of the period. An attempt was made to establish some connection between the asymmetric nature of the lines, maximum to red or violet, and the position in the period, but nothing definite

was obtained. It is evident, however, that a very slight shift of the position of the maximum, one indeed that would scarcely be noticed in the broad and diffuse lines of this spectrum, would be quite sufficient to account for residuals of the magnitude present on each side of apastron. Such a shift of the maximum might reasonably be assigned to some physical change in the star's atmosphere without the necessity of considering the secondary curve to be due to any deviations from an elliptic orbit caused by the presence of a third body. These, how-

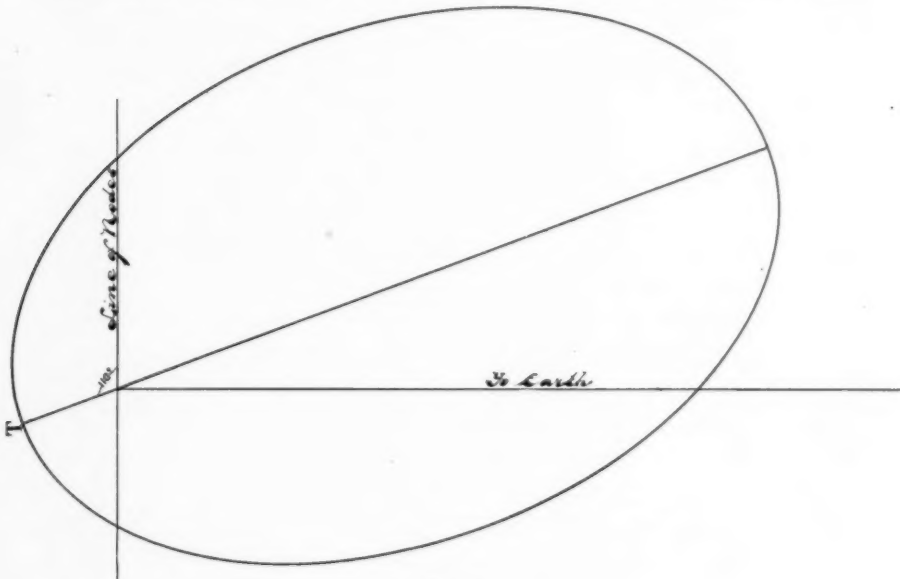


FIG. 2

ever, are speculations which cannot from the data available become anything more.

The remaining elements of the orbit are easily obtained by the well-known methods where, as here, the values of U , e , ω , K , and T are known.

U , or Period,	$= 29.136$ days
e	$= 0.75$
ω	$= 110^\circ$
A, or Positive Maximum,	$= +104$ km
B, or Negative Maximum,	$= -120$ km
K	$= 112$ km

$T = 1.94$ days	= Julian day 2,417,587.94
γ , or velocity of system,	= +20.7 km
$a \sin i$	= 29,680.000 km

A diagram of the orbit showing the proportions of the system is given in Fig. 2.

It is with much pleasure that the advice and encouragement given by the Director, Dr. W. F. King, in the progress of the work are hereby acknowledged.

DOMINION OBSERVATORY

OTTAWA, CANADA

February 1908

ON THE ZONAL ERRORS IN MAGNIFICATION OF THE REFLECTING TELESCOPE

By ARTHUR C. LUNN

It is known that in the case of the reflecting telescope in any of its usual forms the principal reason for the smallness of the field of good definition is the presence of coma in the extra-axial point-images, which, if the axial image is well defined, is to be ascribed to the fact that an areal image surrounding the axis is differently magnified by the different zones of the mirror or mirror-system. Abbe, who gave this explanation for the general case of any optical instrument consisting of a centered system of reflecting or refracting surfaces of revolution, showed that the magnification by any zone is

$$m = \frac{\sin u'}{\sin u}, \quad (1)$$

where u' and u are the angles made with the axis by conjugate rays of a central pencil, respectively before and after passage through the zone in question.¹ If the object is at infinity, as in the astronomical case, $\sin u'$ is to be replaced by the linear distance from the axis to the parallel ray incident on that zone, then m will give the ratio of the size of the image to that yielded by an ideal objective of unit focal length. Good definition in the neighborhood of the axis demands the constancy of m for all zones of the aperture, which is the famous "sine-condition" of optical design.

The corresponding errors in the refracting telescope can be removed over a field of a certain size by appropriate design of the component lenses, as in the telescopes used for the astrographic chart and in general those having objectives of the Fraunhofer type. Here the four (or more) refracting surfaces, while so nearly spherical as to be individually far from aberration-free, have their curvatures so chosen that when combined they give the required compensation of their indi-

¹ Czapski-Eppenstein, *Grundzüge der Theorie der optischen Instrumente nach Abbe*, pp. 123 ff.

vidual errors of magnification, simultaneously with a complete or approximate compensation of their axial aberrations, leaving perhaps a residue of the latter to be removed by slight departures from the spherical figures.

There is no theoretical reason why such a compensation could not be effected in the case of a reflecting telescope, consisting of two or more mirrors with their meridian curves so designed that while the individual reflections would in general not be free from aberration on the axis, yet the system as a whole would yield a perfectly defined axial image and at the same time satisfy the sine-condition. An example of such a system has been described by Schwarzschild,¹ consisting of a pair of mirrors resembling the Cassegrainian form, each of which is, for a considerable angular aperture, so nearly a quadric surface of revolution as to admit of separate testing by the use of its geometric foci as optically conjugate; but in neither case are these the conjugate foci proper to the mirror when combined into the system.

For convenience of testing and other reasons it is however desirable, and in existing constructions apparently universal, for each mirror separately to be free from axial aberration through being a quadric surface of revolution having as conjugate optical foci its own geometric foci. The present investigation concerns the question: How far is it possible by suitable choice of the focal lengths of the component mirrors, retaining this practical condition, to diminish the errors due to the departures from constancy of the sine-ratio? The outcome is that for all such systems, of any number of mirrors, those errors are essentially the same, and identical with those pertaining to a simple parabolic mirror of equivalent relative aperture and focal length; so that for any essential improvement of extra-axial definition in this sense, without sacrifice of the illumination of the image through diminution of the effective angular aperture, the condition that each mirror be separately corrected for aberration must be given up.

To find the value of m for a single mirror let e be the eccentricity of the conic section which is its meridian curve; and for definiteness suppose first that this curve is an ellipse of major semi-axis a , and

¹ *Abhandlungen der k. Gesellschaft der Wissenschaften zu Göttingen, Math. Phys. Klasse, Neue Folge, Band IV, No. 2, 1905.*

that an axial pencil is reflected from the farther to the nearer focus at a point of the mirror whose respective distances from the foci are r' , r .

If the angles u' , u be taken to be acute and of the same sign when the point of reflection is between the vertex of the mirror and the cross-section through the nearer focus, the geometry of the ellipse gives

$$ae + r \cos u = -ae + r' \cos u', \quad r \sin u = r' \sin u', \quad r + r' = 2a, \quad (2)$$

from which by elimination of r , r' comes

$$e = \frac{\sin(u - u')}{\sin u + \sin u'}. \quad (3)$$

If u' be eliminated from this equation by means of the relations

$$\sin u' = m \sin u, \quad \sin^2 u' + \cos^2 u' = 1,$$

there results the quadratic equation for m :

$$m^2(1 + 2e \cos u + e^2) + 2me(e + \cos u) - (1 - e^2) = 0.$$

The root -1 is not applicable, being introduced by multiplication by $\sin u + \sin u'$, hence

$$m = \frac{1 - e^2}{1 + 2e \cos u + e^2}. \quad (4)$$

A similar deduction shows that equations (3) and (4) apply without change also to the case of the hyperbola, provided that the angles u' , u be taken then as having opposite signs, corresponding to the fact that the conjugate foci lie on opposite sides of the mirror, while for the ellipse they are on the same side. This distinction is suitable also for the reason that with the ellipse, for which m is positive, the image and object are inverted with respect to each other, while in the case of the hyperbola, where m is negative, they are relatively erect. Moreover, equation (3) shows that interchange of u and u' simply changes the sign of e , so that the case of reflection from the nearer to the farther focus is accounted for by making e then negative. With these conventions, equation (4) may be regarded as the general expression for the zonal variation of the magnification in terms of the angle u between the axis and the ray after reflection. Since, however, the absolute value of the magnification is not important for the present purpose, but only its relative variations for different zones, it is more convenient to use the ratio of m to the paraxial or ideal magnifi-

cation m_o , the latter being the limiting value of m as u approaches zero, which by (4) is

$$m_o = \lim_{u \rightarrow 0} \frac{\sin u'}{\sin u} = \frac{1-e}{1+e}, \quad (5)$$

so that

$$M = \frac{m}{m_o} = \left\{ 1 - \frac{4e}{(1+e)^2} \sin^2 \frac{u}{2} \right\}^{-1}, \quad (6)$$

a formula which has the advantage of being directly applicable without indeterminateness also to the intermediate case $e=1$, or the parabolic mirror, for which the factor M is analogous to the "blurring factor" defined by Schaeberle¹ and tabulated by him for the extreme aperture of certain important instruments. For all values of u likely to occur in practice with a mirror of given eccentricity e , the value of M may be expanded as a rapidly converging series in even powers of u :

$$M = 1 + \frac{e}{(1+e)^2} u^2 + \dots \quad (7)$$

where the term in u^2 measures the zonal error of the first order, by far the most important in ordinary cases.

Consider next a system of two mirrors, denoted in optical order by indices 1, 2, respectively, so that $u'_2 = u'_1$. Then the paraxial magnification is

$$m_o = \frac{1-e_1}{1+e_1} \cdot \frac{1-e_2}{1+e_2}, \quad (8)$$

so that in this regard the system is equivalent to a single mirror of eccentricity e , defined by

$$\frac{1-e}{1+e} = \frac{1-e_1}{1+e_1} \cdot \frac{1-e_2}{1+e_2}, \quad (9)$$

whence

$$e = \frac{e_1 + e_2}{1 + e_1 e_2}. \quad (10)$$

The zonal factor for the first mirror is

$$M_1 = \left\{ 1 - \frac{4e_1}{(1+e_1)^2} \sin^2 \frac{u_1}{2} \right\}^{-1}, \quad (11)$$

while, since interchange of foci changes the sign of the eccentricity and changes the magnification to its reciprocal, the similar factor for the second mirror can be written

$$M_2 = 1 + \frac{4e_2}{(1-e_2)^2} \sin^2 \frac{u_1}{2}. \quad (12)$$

¹ *Astronomical Journal*, 18, 35, 1897.

Elimination of u_1 from these two equations gives the relation

$$M_1 = \left\{ 1 - \frac{e_1(1-e_2)^2}{e_2(1+e_1)^2} [M_2 - 1] \right\}^{-1}, \quad (13)$$

which is an identity for all zones of the aperture. But M_2 is given also by

$$M_2 = \left\{ 1 - \frac{4e_2}{(1+e_2)^2} \sin^2 \frac{u_2}{2} \right\}^{-1}. \quad (14)$$

Hence the zonal factor for the system is

$$M = M_1 M_2 = \left\{ 1 - \frac{4[e_1(1+e_2)^2 + e_2(1+e_1)^2]}{(1+e_1)^2(1+e_2)^2} \cdot \sin^2 \frac{u_2}{2} \right\}^{-1}, \quad (15)$$

which according to (10) can be written

$$M = \left\{ 1 - \frac{4e}{(1+e)^2} \sin^2 \frac{u_2}{2} \right\}^{-1} \quad (16)$$

in form similar to (6). This shows that the single substitute mirror of eccentricity determined according to (10) by the paraxial magnification is equivalent to the system also in its zonal errors. By induction it follows that a system of n mirrors can be replaced in the same sense by a single equivalent mirror of eccentricity defined by

$$\frac{1-e}{1+e} = \prod_{i=1}^n \frac{1-e_i}{1+e_i}. \quad (17)$$

The proof would need to be modified to cover the cases where e as thus defined becomes indeterminate, but these are of no practical importance.

In any optical combination consisting of a centered system of reflecting surfaces of revolution, each of which is individually corrected for axial aberration, the relative zonal errors of magnification at given points in the final angular aperture are identical with those of a single mirror giving the same paraxial magnification.

In the astronomical case the eccentricity of the first mirror is unity, and the definition of paraxial magnification must be modified accordingly; but equation (17) makes the substitute mirror also parabolic, as it should, and with e so defined the proof for the zonal factor M remains valid, so that the system is equivalent to a simple parabolic mirror of the same linear aperture and focal length. From the present point of view the advantage of the Gregorian and more especially of

the Cassegrainian form of telescope over the Newtonian lies in the increased focal length and consequently diminished angular aperture attainable, with a principal mirror of given linear aperture and a mounting of given size.

CHICAGO, ILLINOIS
February 1908

THE DETERMINATION OF THE HELIOCENTRIC POSITION OF A CERTAIN CLASS OF CORONAL STREAMERS¹

BY JOHN A. MILLER

In his *Mechanical Theory of the Sun's Corona*, Professor Schaeberle assumes that the theoretical corona is caused by light emitted and reflected from streams of matter ejected from the sun by forces, which in general act along lines normal to its surface. These streams are assumed to be formed of a series of particles ejected from the same point of the sun's surface and following each other in such a way that they make a continuous stream. From the laws of mechanics it follows, as Professor Schaeberle points out, that of two particles of the same stream, that particle has the less angular velocity which is at the greater distance from the sun's surface. He further assumes that the streamers which we see are not the actual streams but *rays* that, because of a certain optical principle, result from the orthographic projection of two or more series of streams that intersect each other at a small angle.

In what follows I have used all these assumptions except the last. Instead, and with no thought of controverting this notable and ingenious explanation of the corona, I have assumed that what we see and photograph are the real streams projected orthographically on a plane perpendicular to a line joining the observer's eye and the center of the sun. Throughout the paper I have used the word *stream* to mean the actual stream of ejected particles and the word *streamer* to mean the orthographic projection of the stream.

If we grant the above assumptions it is possible to show that some of these streamers will curve away from the projection of the pole of the sun throughout their entire length, some will curve toward it, while a few of them will at first curve away from, and later toward it, or vice versa. For the latter class of streamers, it is possible to find the heliocentric latitude and longitude of a particle at that part

¹ It is a pleasure to acknowledge my obligations to Mr. Walter R. Marriott, instructor in mathematics, Swarthmore College, who has aided me in many ways, but particularly with the rather tedious computations.

of the streamer where it reverses its direction of curvature, the distance of this particle from the sun, the point on the sun's surface from which the particle was ejected, the time it was ejected, and hence the position of the point of ejection at any time; we can also find the velocity with which the particle was ejected, the velocity of the particle at any time, the orbit of each particle in the stream, and the resultant of all forces acting on the particle, and, if we assume the law of the force, we can find the magnitude of any repulsive force, such as light or electric pressure, that may exist. It is further possible to find a rough approximation of the position of streamers of the first two classes.

To prove these assertions, choose as

z -axis, the axis of the sun;

x -axis, the equatorial diameter passing through the west side of the sun;

y -axis, a line perpendicular to the xz -plane.

Let x, y, z be the rectangular heliocentric co-ordinates of any point;

Let ϕ be its heliocentric latitude;

Let θ be its heliocentric longitude, measured from the yz -plane, positive in the direction of the sun's rotation;

Let R be its radius vector;

Let λ be the angle between the z -axis and the line through the observer and the center of the sun;

Let the x - and the z -axis project into a ξ - and η -axis respectively;

Let A be the angle that the projection of a radial line makes with the ξ -axis.

Then,

$$\left. \begin{aligned} x &= R \cos \phi \sin \theta, \\ y &= R \cos \phi \cos \theta, \\ z &= R \sin \phi. \end{aligned} \right\} \quad (1)$$

$$\begin{aligned} \xi &= x, \\ \eta &= z \sin \lambda - y \cos \lambda, \end{aligned} \quad (2)$$

$$\tan A = \frac{\sin \lambda \tan \phi - \cos \lambda \cos \theta}{\sin \theta}. \quad (3)$$

Hence all points lying in the plane

$$\tan \lambda \tan \phi - \cos \theta = 0$$

will project into the ξ -axis.

All points lying in the plane

$$\cos \phi \sin \theta \tan A - \sin \lambda \sin \phi + \cos \lambda \cos \phi \cos \theta = 0$$

will project into a straight line, making an angle A with the ξ -axis. The equation of the line will be

$$\eta - \tan A \cdot \xi = 0.$$

If the force of ejection is normal to the surface of the sun, an ejected particle will move in the plane of a great circle perpendicular to the meridian of the sun through the point of ejection at the time of ejection and tangent to the small circle described by the point of ejection. Hence $\tan A$ will in general be different for different parts of the same streamer. For, let

t_0 =time of ejection,

θ_0 =longitude of P_0 , the point of ejection at the time of t_0 ,

ϕ_0 =latitude of P_0 at the time t_0 ,

ϕ =latitude of the ejected particle P at any time t ,

θ =longitude of P at any time t ,

ρ =the projection of the radius vector of P .

Let P'' be the pole of the sun.

Then from the spherical triangle $P_0P''P$

$$\cos(\theta - \theta_0) \tan \phi_0 = \tan \phi \quad (a)$$

hence

$$-\sin(\theta - \theta_0) \tan \phi_0 = \frac{d}{d\theta} (\tan \phi). \quad (b)$$

We may differentiate (3) with regard to θ , and by the aid of (b) express

$$\frac{d}{d\theta} (\tan A)$$

as a function of θ and constants. If

$$\frac{d}{d\theta} (\tan A) \equiv 0,$$

the streamer will be a straight line and in this case only. In all other cases $\tan A$ will change, that is, the streamer will curve; for the θ is different for different parts of the stream.

It is at once evident that one, in a rough way, can locate any curved streamer or curved prominence if the curvature is due to the rotation of the sun. Or, better expressed, one can determine whether or not a given streamer comes from a certain large region of the sun. For on any stream the longitude of the points decreases as the distance from the sun increases and $\tan A$ increases or decreases with θ

according as $\frac{d}{d\theta}(\tan A)$ is positive or negative. Hence if $\tan A$ is positive and $\frac{d}{d\theta}(\tan A)$ is positive, the streamer curves away from the pole. If, on the other hand, $\tan A$ is positive and $\frac{d}{d\theta}(\tan A)$ is negative, the streamer curves toward the pole. That is, if the streamer curves away from the pole, θ and ϕ must satisfy equation (3) and the inequality $\frac{d}{d\theta}(\tan A) > 0$. On the other hand, if the streamer curves toward the pole, θ and ϕ must satisfy equation (3) and the inequality $\frac{d}{d\theta}(\tan A) < 0$. If one selects from the regions thus limited those regions from which streams visible during an eclipse may issue, he may obtain in many instances fairly approximate values of θ and ϕ . If one makes the further assumption (not far from the truth in low latitudes) that $\frac{d}{d\theta}(\tan \phi) = 0$ there results the very simple form,

$$\frac{d}{d\theta}(\tan A) = \frac{\cos \lambda - \sin \lambda \tan \phi \cos \theta}{\sin^2 \theta}.$$

The position of streamers of the third class, that is, those that for a part of their length curve away from the pole and for the remainder of their length toward it, may be found exactly. For $\tan A$ increases (or decreases) for a part of the streamer and then decreases (or increases) for the remainder if, and only if, $\frac{d}{d\theta}(\tan A)$ changes sign; that is, passes through infinity or zero. $\frac{d}{d\theta}(\tan A)$ passes through infinity if $\tan \phi = \infty$, or $\sin \theta = 0$; that is, for streams at pole of the sun or in the yz -plane. In either case $A = 90^\circ$. Hence θ and ϕ for the point of a streamer where it reverses its direction of curvature satisfy the equation $\frac{d}{d\theta}(\tan A) = 0$.

Solving this equation simultaneously with (3), (a), and (b), we get

$$\tan \theta = \frac{\tan A + \cos \lambda \tan(\theta - \theta_0)}{\cos \lambda - \tan A \tan(\theta - \theta_0)} \quad (4)$$

$$\tan \phi = \frac{\cot \lambda}{\sin \theta \tan(\theta - \theta_0) + \cos \theta}. \quad (5)$$

Projecting R on the ξ -axis we have

$$R = \frac{\rho \cos A}{\cos \phi \sin \theta} \quad (6)$$

A and ρ can be measured on the photograph, and hence equations (4), (5), and (6) determine exactly the heliocentric position and the radius vector of the point in a streamer where it reverses its direction of curvature provided we can find $\theta - \theta_0$.

I have assumed that the force of ejection is normal to the sun's surface, and therefore, because of the velocity imparted to the particle by the sun's rotation, the direction of the initial velocity will not be along a normal to the sun. I have assumed also that after the particle is ejected the resultant of all forces acting on it—the sun's attraction and light or electric pressure—is a central force passing through the center of the sun and that it varies inversely as the square of the distance from the center. Each particle of the stream will therefore describe an ellipse,¹ one focus of which—the one near perihelion—will be the center of the sun. It seems reasonable to suppose that all the particles of the stream have been ejected with the same velocity, and, since they are issuing from the same point on the sun, the major axis and the eccentricity of the orbits of all the particles are equal, though the planes of the orbits are different.

It is necessary to measure, in addition to A and ρ , $a(1+e)$, the greatest distance from the center of the sun that the stream attains. Before this is possible θ and ϕ must be approximately known, since the projection of $a(1+e)$ is all that we can measure. A first approximation of the values of θ and ϕ may be obtained by assuming that

$$\frac{d}{d\theta} (\tan \phi) = 0.$$

With this assumption (4) and (5) become

$$\tan \theta = \frac{\tan A}{\cos \lambda} \quad (4')$$

$$\tan \phi = \frac{\cot \lambda}{\cos \theta}. \quad (5')$$

The value that one obtains of $a(1+e)$ is somewhat uncertain. A definite minimum value may be assigned to it since it cannot be less than its measured value. Its maximum value, however, is much

¹ Or parabola or hyperbola. The curves on the plate discussed later are ellipses.

less definite. The stream may not have reached its greatest height or the entire stream may not have been photographed. However, all streamers broaden as they recede from the sun and the abrupt curvature of many streamers near their upper extension leads one to believe that he may be guided somewhat by the shape of the streamer and that he can assign a reasonably definite maximum limit. Besides, as can be easily verified by computation, one can change $a(1+e)$ within fairly large limits without affecting large changes in θ and ϕ .

To complete the solution,

Let P be a particle at that point of the streamer where the curvature reverses its direction;

Let P_o be the point on the sun from which P was ejected;

Let P' be a particle at any point in the streamer;

Let P'_o be the point of ejection of P' ;

Let t be the time at which the photograph was made;

Let t_o and t'_o be the time when P and P' left the sun respectively;

Let θ, ϕ, R, w =respectively, the longitude, latitude, radius vector, and true anomaly of P at the time of t ;

Let $\theta_o, \phi_o, R_o, w_o$ =respectively like values for P_o at time t_o ;

Let θ', ϕ', R', w' =respectively like values for P' at time t' ;

Let $\theta'_o, \phi'_o, R'_o, w'_o$ =respectively like values for P'_o at time t'_o ;

Let v_s =velocity of ejection;

Let v_r =velocity of the particle due to the sun's rotation;

Let V =velocity with which the particle left the sun;

Let e =eccentricity of the orbits;

Let a =semimajor axis of the orbits;

Let ω =angular velocity of the sun;

Let n =the mean motion in the orbit;

Let C^2 =the constant entering into the differential equations of motion;

Let ψ =angle between the normal to the sun and the initial velocity.

In addition to equations (4), (5), and (6) we have from spherical triangles,

$$\tan(\theta - \theta_o) = \frac{\tan(w - w_o)}{\cos \phi_o} \quad (7)$$

$$\tan(\theta' - \theta_o) = \frac{\tan(w' - w'_o)}{\cos \phi_o} \quad (8)$$

$$\tan \phi_o = \frac{\tan \phi}{\tan(\theta - \theta_o)}. \quad (9)$$

Now a large change in θ produces a small change in ϕ except in very high latitudes. Hence if we choose for P' the point in the streamer at the edge of moon's shadow, we can without sensible error put $\phi' = \phi_0$. Substituting this value of ϕ' in (3) we may solve for θ' . We may now solve for R' . Since the particles travel in ellipses we have,

$$R = \frac{a(1-e^2)}{1+e \cos w} \quad (10)$$

Since four values of R are known, (10) yields four equations. Also

$$a(1+e) = \text{some measured quantity}, \quad (11)$$

$$t - t_0 = \int_{R_0}^R \frac{R}{a\sqrt{(a^2e^2 - (a-R)^2)}} dR \quad (12)$$

This yields two equations.

We have also

$$n^2a^3 = C^2 \quad (13)$$

$$\tan \psi = \frac{v_1}{v_2}$$

$$4a^2e^2 = R_0^2 + (2a - R_0)^2 + 2R_0(2a - R_0) \cos 2\psi \quad (14)$$

$$V_1 = \omega R_0 \cos \phi_0 \quad (15)$$

$$v_1^2 + v_2^2 = V^2$$

$$V^2 = C^2 \left[\frac{2}{R_0} - \frac{1}{a} \right] \quad (16)$$

$$\theta'_0 - \theta_0 = \omega(t'_0 - t_0). \quad (17)$$

This is a sufficient number of equations to solve the problem completely.

I have made an application of the preceding theory to the large-scale photographs made by Professor W. A. Cogshall and myself at Almazan, Spain, during the total solar eclipse of August 30, 1905. These photographs were made with a lens of nine inches aperture and sixty feet focal length, mounted with its axis horizontal; the light being reflected into it by means of a coelostat. The weather on the day of the eclipse was disappointing. For two hours before totality the entire sky was covered with light though unbroken clouds. At the time of totality, however, the clouds in the immediate vicinity of the sun appeared to break away and the inner corona shone through light drifting clouds. The photographs show a very great deal of coronal detail, though they lack some of the definiteness that would have come from good seeing. The clouds made it impossible

to register very long streamers—the longest one photographed being about three-fourths that of the sun's diameter.

From the negative made near the time of mid-totality, a series of positives was made, each positive being printed deeper than the preceding one. On the thinnest positives the detail near the sun was lost, while on the densest positives the detail at a short distance from the sun was printed out. By the aid of this series it was possible to trace a given streamer throughout its entire length.

The general appearance of the corona over the region of the great prominences on the eastern limb of the sun indicates a very complex structure. The streamers there are not radial and their directions away from the sun are so random as compared with simpler structure at other places that one can hardly escape the impression that they have been influenced by the prominences. Practically all the streamers curve, and curve regularly, though not uniformly. Most of them are nearly radial near the base, and curve much less rapidly there than at some distance from the sun, qualitatively, at least, as a stream of matter ejected from the sun would do. The diameter of nearly every streamer is smaller near the base than at the top. Of 63 streamers, which were all that seemed to me to be well defined, the bases of 18 were inclined north of the center of the sun and the bases of 6 were inclined south of the center; 39 curve toward the equator, and 14 away from it. The remaining ones, so far as I could tell, were perfectly straight.

In addition to these I found five streamers—four on the west, and one on the east margin of the sun—that had double curvature. All curved first away from the pole, then toward it. I chose three of these streamers, all on the west limb of the sun, for discussion. Two of them were apparently near each other, the remaining one separated some distance from these. Denote by A and A' , respectively, the angle A where the streamer reverses its direction of curvature (in our case where the streamer begins to curve toward the pole) and where the streamer meets the margin of the shadow. I measured these angles with a protractor that read to minutes, setting the protractor five times and measuring the angle four times at each setting. The table below contains the means of these measures as well as those of ρ .

Streamer	No. 1	No. 2	No. 3
A	$2^\circ 25'$	$11^\circ 09'$	$59^\circ 38'$
A'	$3^\circ 34'$	$12^\circ 45'$	$62^\circ 27'$
ρ	$4\frac{1}{4} R_\odot$	$4\frac{1}{4} R_\odot$	$4\frac{1}{4} R_\odot$

Computing λ we find

$$\lambda = 84^\circ 42'.$$

Using formulas (4'), (5'), and (6) we find the following approximate values:

Streamer	No. 1	No. 2	No. 3
θ	$24^\circ 33' 20''$	$64^\circ 53' 24''$	$86^\circ 54' 07''$
ϕ	$5^\circ 49' 25''$	$12^\circ 19' 52''$	$59^\circ 46' 35''$
R	$2.574 R_\odot$	$1.271 R_\odot$	$1.183 R_\odot$

These values must be regarded as very rough approximations.

The values that one may now obtain for $t-t_0$ and for θ' show beyond question either that the assumptions that were made regarding the formation of the streams were wrong, or that some other force than the attraction of the sun was acting on the particle after its ejection and that this force is a repulsive force. Choosing the latter alternative, we assumed that whatever this force may be its magnitude varies inversely as the square of the distance of the particle from the sun, and treated rigorously streamer No. 1, according to the methods developed in this paper. For this streamer we have the following data:

$$\begin{aligned}A &= 2^\circ 25', \\A' &= 3^\circ 34', \\ \rho &= 4\frac{1}{4} R_\odot, \\ a(1+e) &= 2.5 R_\odot.\end{aligned}$$

Solving equations (3) to (17) we get the following values:

$$\begin{aligned}\theta &= 54^\circ 33', \quad \theta' = 58^\circ 19', \quad a = 1.635 R_\odot, \quad \phi_0 = 5^\circ 49' 22'', \\ \phi &= 5^\circ 02' 49'', \quad \phi' = 5^\circ 49' 22'', \quad e = 0.529, \quad t - t_0 = 251,860 \text{ seconds}, \\ R &= 1.314 R_\odot, \quad R' = 1.179, \quad \theta_0 = 24^\circ 33', \quad v_s = 0.6 \text{ miles per second}.\end{aligned}$$

The repulsive force is 0.99 the attraction of the sun.

That is, the particle P at the point of the streamer where it reverses its direction of curvature left the sun 251,860 seconds before the eclipse occurred. The longitude and the latitude of the point of ejection when the particle was ejected were $24^\circ 33'$ and $5^\circ 49' 22''$

respectively. At the time of the eclipse P was 1.3 radii of the sun from its center.

The force of repulsion is surprisingly large and hence the velocity of ejection very small. These results are entirely consistent with the conclusions reached by Campbell and Perrine (*L. O. Bulletin* No. 115), and confirm in a measure the conclusions of Arrhenius (*L. O. Bulletin* No. 58).

One cannot draw general conclusions from one plate or one streamer, but the nature of these results is such as to warrant the reduction of others of the numerous large-scale photographs of the solar corona made since 1893.

SWARTHMORE COLLEGE

SWARTHMORE, PA.

March 21, 1908

METALLIC ARCS FOR SPECTROSCOPIC INVESTIGATIONS

BY A. H. PFUND

In connection with some work which I have been doing recently on the redetermination of the wave-lengths of the iron lines according to the method of Fabry and Perot, it has been found not only desirable but imperative that the iron arc should burn steadily, without wandering or flickering. If one may judge from the most recent literature on the subject,¹ it is considered most difficult, if not impossible, to realize this condition for any desired length of time. Recently, however, I have constructed a simple type of iron arc which burns with an almost perfect steadiness and without the least attention for an hour or more. As the iron arc is so universally employed in spectroscopy, and as this new construction makes it a pleasure instead of a burden to work with this type of arc, I have thought it worth while to present the following note on the subject.

Although the iron arc usually jumps about in a most erratic manner, it does occasionally settle down and burn steadily. If, at such a time, the arc be viewed through a piece of smoked glass, it is found that the discharge proceeds from a bead of molten iron oxide on the lower electrode and terminates on a small bright patch on the upper electrode. This upper electrode, if it form the negative pole, becomes hollowed out in time to form a crater. The difficulty with this arrangement is that the bead of molten iron oxide soon rolls off the electrode and the wandering of the arc once more sets in. In order to realize permanently the conditions which existed while the arc was burning steadily, the construction shown in Fig. 1 was adopted.

The lower (positive) electrode (*a*), consisting of a rod of iron about 12 mm in diameter, carries a bead of iron oxide (*b*) in a small cup-shaped bowl. The upper electrode (*c*), an iron rod about 6 mm in diameter, is made to project by 3 mm from a brass bushing (*d*) fastened to the rod by a set-screw (*e*). This is done to prevent the electrode from getting too hot. Such an arc burns best if sup-

¹ P. Eversheim, *Astrophysical Journal*, 26, 172, 1907; *Zeitschrift für wiss. Photographie*, 5, 152, 1907.

plied with about 3.5 amperes from a 220-volt direct-current circuit. After the electrodes are carefully centered, the arc can usually be started by bringing the two electrodes into contact and then separating them. If this fails, the desired result can be brought about by bridging the gap between the electrodes by means of a carbon rod, or by heating the bead of oxide to red heat by means of a Bunsen burner and then bringing the electrodes into contact. It is best to limit the length of arc to about 6 mm. After burning for an hour or more, the upper electrode becomes incrusted with a layer of iron oxide which forms the crater already alluded to. Before starting the arc anew it is best to knock off this crust and to readjust the brass bushing.

In attempting to apply this same construction to arcs of other metals it was found, as for example in the case of copper, that if the upper electrode were also made of copper the arc behaved very badly. Therefore the following general construction was adopted, which works perfectly for the metals thus far tried, viz., iron, nickel, cobalt, copper, silver, and platinum. The iron rod already described forms the lower (positive) electrode while a rod of carbon about 1 cm in diameter forms the upper electrode. In order to produce a copper arc a bead of copper oxide is placed on the lower electrode and the arc is started. Having prepared beads of the different metals or their oxides and having placed these beads in properly labeled pill-boxes, all that is necessary to change from, say, the copper arc to the nickel arc is remove the copper bead by means of a pair of tweezers and to replace it by a nickel bead. The method is as simple as it is satisfactory.

A bead of any metal may be made by placing a small piece of the metal in question on the lower electrode. Upon starting the arc, the bead is formed immediately. If it is found that the bead is too small, its size can be increased by feeding some wire of the same metal into the bead while the arc is burning. The bead ought to be about 3 mm in diameter. It is to be emphasized in this connection that the condition essential to the proper behavior of the arc

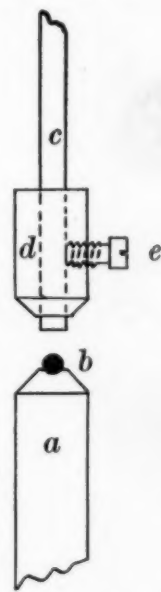


FIG. 1

is that the bead of molten metal or oxide be in the spheroidal state and that it bulge out considerably above the edges of its receptacle—as is shown in Fig. 1.

Of the various metals tried, the only one which at first gave trouble was silver. It was found that a bead of silver when placed upon the 12 mm iron rod failed to melt—and in consequence the arc was not steady. By using a carbon rod in place of the iron, this silver bead became as fluid as water and shot out minute globules of metallic silver. The proper conditions, which evidently lay between these two extremes, were finally realized by placing the bead on a rod of iron but 7 mm in diameter. This rod became sufficiently hot to keep the silver in a molten condition without getting it too hot. Under these conditions the arc behaves perfectly. In the case of platinum either a carbon or a thin iron rod may be used.

These arcs, in which carbon is used as one electrode, may be drawn out to the length of about an inch and still behave satisfactorily. The current may also be increased beyond 3.5 amperes. Comparing the spectrum of the iron arc produced when the upper electrode is of iron with that produced when the upper electrode is of carbon, it is found (as has been known before) that in the latter case the spectrum is very much weaker and that the lines in the visible region are relatively more weakened than those in the ultra-violet. A study of the Fabry and Perot fringe system shows that the lines produced by this carbon-iron arc rival in homogeneity and sharpness the red and green lines of cadmium produced in a vacuum arc.

JOHNS HOPKINS UNIVERSITY
March 1908

A NEW MERCURY LAMP

By A. H. PFUND

The following is the description of a simple form of mercury vapor arc, adapted for use in the visible as well as the ultra-violet spectrum and capable of being made by anyone familiar with the rudiments of glass-blowing. As will be seen from Fig. 1, the lamp consists of a piece of glass tubing about 7 cm in length and 1.2 cm

in diameter, to which there is sealed a larger tube, 3 cm in diameter and 18 cm in length. A side tube is sealed on this larger portion for the purpose of exhaustion. A platinum wire is sealed into the lower end of the smaller tube, which is then filled with clean mercury to a height of about 3 cm. The mercury forms the negative electrode, while a hollow sheet-iron electrode forms the positive. This electrode is made by cutting out a piece of sheet-iron as shown in Fig. 2 (a) which is subsequently bent into the form shown in Fig. 2 (b). The lower portion of this electrode is of somewhat smaller diameter than the upper, and, when in place, does not touch the glass tube at any point. This construction is adopted for the reason that the arc, which terminates on the lower ring of this electrode, raises it to red heat—and if this portion of the electrode were in contact with the glass, a crack would result. The positive electrode is about 1 cm above the mercury and is held in place by friction. The current is led into this electrode by means of an iron wire passing along the length of the tube and out at the top. As the iron wire is considerably heated by the current and as under these conditions there is a tendency to soften the sealing-wax, through which this wire passes, it

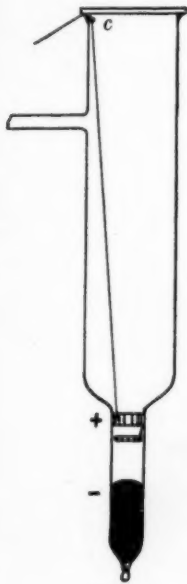


FIG. 1

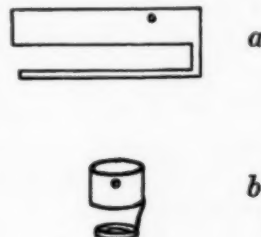


FIG. 2

is advisable to fuse a piece of copper wire to the iron, as shown in Fig. 1 at (c). The copper wire must be shellaced thoroughly to keep it from being amalgamated. The top of the lamp is closed by a quartz plate, the air-tight seal being effected by means of sealing-wax.

The lamp is next exhausted on a mercury air-pump and it is best to run and heat the lamp while it is still on the pump so as to drive off the water vapor and the gases contained in the electrodes. After carrying the exhaustion to as high a degree as possible, the lamp is sealed off from the pump and is ready for use.

The lamp burns in a vertical position and consumes from 1.4 to 1.6 amperes supplied from a 110-volt direct-current circuit. The arc is readily started by heating the lower, mercury-filled portion by means of a Bunsen burner. Either by tilting the lamp or by giving it a sudden, upward jerk, contact is made between the two electrodes and the discharge sets in. If the light in the visible spectrum alone is required, it may be taken out through the side of the tube, but if the ultra-violet is also needed, it is taken out through the quartz window at the top. A totally reflecting quartz prism or a speculum mirror gives the light a horizontal direction.

After the lamp has been running for several days it is found that gases are liberated and as a result the arc becomes so hot that the glass softens and eventually sucks in. It is easy, however, to avoid this by testing, from time to time, whether the glass is getting too hot. If paper, upon being held against the glass, is charred, it is time to stop the discharge and to re-exhaust.

Without discussing in detail the various advantages of this type of mercury lamp, it may be stated that the lamp lasts for a long time and that, without applying strips of wet cloth to the upper portion of the large tube, it remains cold and no mercury condenses on the quartz window.

JOHNS HOPKINS UNIVERSITY
March 1908